

# Global Optimization of Gas Transportation and Storage: Convex Hull Characterizations and Relaxations

Bahar Cennet Okumuşoğlu <sup>1</sup> and Burak Kocuk <sup>2</sup>

<sup>1</sup>TUM School of Management, Technical University of Munich, 80333, Munich, Germany.

<sup>2</sup>Industrial Engineering Program, Sabancı University, 34956, Istanbul, Turkey.

Contributing authors: [bahar.okumusoglu@tum.de](mailto:bahar.okumusoglu@tum.de); [burak.kocuk@sabanciuniv.edu](mailto:burak.kocuk@sabanciuniv.edu);

## Abstract

Gas transportation and storage has become one of the most relevant and important optimization problem in energy systems. This problem inherently includes highly nonlinear and nonconvex aspects due to gas physics, and discrete aspects due to control decisions of active network elements. Obtaining locally feasible or global solutions for this problem presents significant mathematical and computational challenges for system operators. In this paper, we formulate this problem as a nonconvex mixed-integer nonlinear program (MINLP) through disjunctions. Moreover, we study the nonconvex sets induced by gas physics and propose mixed-integer second-order cone programming relaxations for the nonconvex MINLP problem. The proposed relaxations are based on the convex hull representations of the nonconvex sets as follows: We give the convex hull representation of the nonconvex set for pipes and show that it is second-order cone representable. We also give a complete characterization of the extreme points of the nonconvex set for compressors and show that the convex hull of the extreme points is power cone representable. For practical applications, we propose a second-order cone outer-approximation for the nonconvex set for compressors. To obtain (near) globally optimal solutions, we develop an algorithmic framework based on our convex hull results. We evaluate our framework through extensive computational experiments on various GasLib networks in comparison with the convex relaxations from the literature and state-of-the-art global solver. Our results highlights the computational efficiency and convergence performance of our convex relaxation method compared to other methods. Moreover, our method also consistently provides (near) global solutions as well as high-quality warm-starting points for local solvers.

**Keywords:** Convex hull, Mixed-integer nonlinear programming, Global optimization, Gas networks

## 1 Introduction

Gas transportation is one of the most important optimization problems in gas network systems. It determines the optimal nodal pressures and gas flows through pipelines while balancing the gas supply and demand with minimum operational costs. In addition, the recent technological developments in the gas industry have highlighted the significant role of gas storage [1]. In this respect, considering storage sites in gas transportation optimization problem has become highly relevant and significant to the system operators. The gas stores provide significant security and flexibility for the network operations as they are the most responsive elements in case of supply disruptions and demand fluctuations. However, there remain certain mathematical and computational challenges in the gas transportation and storage problem summarized as follows:

- (i) **Nonlinear and nonconvex relations:** The pressure loss in pipes and the fuel consumption of compressors are described by highly challenging nonconvex and nonlinear equations governed by the laws of physics.
- (ii) **Discrete decisions:** Control decisions of active network elements and bidirectional gas flows require disjunctive formulations and binary decision variables.
- (iii) **Multi-period structure:** Gas injection and withdrawal rates for stores and switching decisions of active network elements necessitate intertemporal constraints.

The gas transportation and storage problem with the aforementioned inherent nonconvex, nonlinear, and discrete aspects belongs to the class of nonconvex mixed-integer nonlinear programming (MINLP) problems. These problems are known to be very hard to solve to optimality as their continuous relaxations still involve nonconvexities.

## 1.1 Literature Review

The gas networks are characterized by the existence of controllable network elements. These networks are called *passive* if they only consist of controllable elements such as pipes and *active* if there also exist controllable elements such as compressors and (control) valves. There is a growing literature on the optimization problems considering different network characteristics as well as their computational complexities (for a recent review, see [2] and references therein). The gas transportation problem in [3] can be efficiently solved in single-source single-sink passive networks, and gas nominations can be decided in polynomial time in single-cycle passive networks [4]. In the existence of active network elements such as compressors and (control) valves, gas network optimization problems are NP-hard. For example, the work by [5] shows that the topology optimization problem in an active gas network is strongly NP-hard. The optimization problems in active gas networks are also known to be practically intractable within the scope of current state-of-the-art global solvers. Therefore, obtaining globally optimal or even locally feasible solutions for optimization problems in active networks is a very challenging task.

Different solution methodologies are applied to solve the gas network optimization problems, which can be categorized into three groups: nonlinear optimization methods, approximation-based approaches, and conic programming relaxations. In nonlinear optimization methods, governing equations can be tackled in their original forms. These methods include sequential linear and quadratic programming [6, 7], interior point methods [8, 9] and primal-relaxed dual decomposition methods [10]. However, these studies do not include active network elements or assume that their control decisions are known a priori. While being able to find locally optimal solutions, these methods provide only a primal bound on the optimal objective value without any optimality guarantees for nonconvex nonlinear problems. Regularization schemes are also applied to nonlinear models with complementarity conditions for discrete aspects [11, 12]. Although the solution approach in [12] is promising to obtain near-global solutions, the authors observe some infeasibility and numerical inaccuracy issues. Also, note that such issues may arise in local methods without acceptable warm starting points.

Approximation-based approaches are widely applied to address nonlinear and nonconvex functions in the literature [13–19]. These approaches are mainly based on piecewise linearizations. Bilinear terms in the nonconvex equations are typically replaced by McCormick inequalities (see, e.g., [18, 20]). Although this approach is commonly used in global optimization, it might result in weak formulations when continuous variables have large bounds. In fact, this is the case for nodal pressure and gas flow bounds in gas network optimization problems. Piecewise linear functions are more successful in approximating inherent nonlinearities that requires the additional of binary variables [12, 18, 21–23]. These piecewise linear approximations lead to mixed-integer linear programming (MILP) models, which are very convenient for the current state-of-the-art commercial solvers. High-resolution solutions produced by these approximations still require many binary variables and MILP formulations might become prohibitively expensive, especially in the presence of discrete control decisions.

Conic programming relaxations have recently attracted attention to deal with nonconvex and nonlinear aspects of gas physics. A semidefinite programming (SDP) relaxation is used to solve the nonconvex equations in a small tree network [24]. Although SDP relaxations are usually tight, they become computationally more expensive as the network size increases. On the other hand, second-order cone programming (SOCP) relaxations have become popular among researchers due to their scalability and exactness under certain assumptions [18, 20, 25–29]. In radial gas networks with known flow directions, pressure loss equations can be relaxed into second-order cone constraints [27]. However, in the more realistic case of arbitrary flow directions, the situation becomes more challenging and necessitates disjunctive constraints. Bidirectional flows are commonly reformulated with flow direction (binary) variables and lead to mixed-integer second-order cone programming (MISOCP) models through big-M formulations [28, 29] and McCormick inequalities [20, 29, 30]. Extended formulations built on perspective functions are also used (see, e.g., [20, 25, 26, 30]). While the proposed relaxations in previous works are computationally tractable, they do not lead to convex hull formulations.

Next, we address the existing gaps in the literature. The optimization problems in gas networks include highly detailed nonlinear, nonconvex, and discrete aspects as mentioned above. Several studies use simplified models and focus on different aspects of these problems. For example, feasible sets for pipes induced by nonconvex pressure equations are commonly approximated by mixed-integer conic sets [20, 25–29]. The novel

work in [20] proposes stronger formulations than previous works under arbitrary gas flows. The authors also emphasize the benefits of MISOCP models. However, the proposed mixed-integer conic sets do not give the convex hull representations of the nonconvex sets for pipes, and the proposed formulations produce weak SOCP relaxations. To approximate the operating domains for compressors simplified models (hereafter referred to as *the feasible set for compressors*) are widely used in the literature [12, 25, 31]. However, the optimization models in active networks also assume idealized compressors, i.e., no fuel consumption [20, 28, 29], or use outer-approximations to preserve convexity [25, 26]. To the best of our knowledge, convex hull descriptions and tight outer-approximations of the feasible sets for these network elements have not been studied in the literature. This paper fills these literature gaps as discussed in the next section.

## 1.2 Our Contributions

In this paper, we aim to find global solutions produced by mixed-integer conic relaxations for the general class of optimization problems in gas networks, including the aforementioned challenges. For this purpose, we study the gas transportation problem and extend it to a multi-period setting with gas stores. We also include the control decisions of active network elements such as compressors and (control) valves. We formulate the gas transportation and storage problem as a nonconvex MINLP. This problem includes highly nonlinear and nonconvex characteristics of the underlying gas physics, namely, two nonconvex feasible sets induced by the nonconvex pressure loss equations for pipes and the fuel consumption equations for compressors. We propose an MISOCP relaxation for this problem by using the convex hull representations of these two nonconvex sets. In particular, our MISOCP relaxation is based on the exact convex hull representation of the feasible set for pipes and the outer-approximation of the convex hull of the feasible set for compressors.

Next, we elaborate on our main contributions:

- **Convexification of the feasible set for pipes:** We focus on the nonconvex feasible set of a single pipe. In Theorem 1, we show that the convex hull of this set is second-order cone representable (SOCr). We also give an extended formulation for the convex hull of this feasible set as Theorem 1 is constructive. To the best of our knowledge, this is the first convex hull formulation of the feasible set for pipes. Moreover, our approach can be extended for those optimization problem that include nonconvex sets with similar characteristics (e.g., water supply networks).
- **Convexification of the feasible set for compressors:** We later focus on the nonconvex feasible set of a single compressor. We give a complete characterization of the extreme points of this nonconvex set, which are not finite. Moreover, we show that the convex hull of the extreme points is power cone representable (POWr) in Theorem 2. To the best of our knowledge, this is the first convex hull characterization of the feasible set for compressors. Moreover, we also propose a mixed-integer second-order cone outer-approximation for this nonconvex set in Theorem 3 since it is not quite practical to solve mixed-integer power cone programs directly using the current state-of-the-art solvers.
- **Algorithmic Developments:** To obtain global or near-global optimal solutions of the problem considered in this paper, we present an algorithmic framework based on our main convex hull results, in particular, Theorems 1, 2 and 3.

We conduct an extensive computational study and compare the proposed framework with the state-of-the-art global solver. We also compare our relaxations with different conic relaxations from the literature under different objective functions. Our computational results show that the proposed framework significantly outperforms the global solver in terms of computational performance and convergence. Our results also illustrate the strength of our conic relaxations in comparison with the relaxations from the literature. Moreover, our approaches offer numerically consistent global and near-global solutions as well as high-quality warm starting points for local solvers.

The rest of the paper is organized as follows: In Section 2, we formally introduce the multi-period gas transportation and storage problem. We present our main results on the (nonconvex) feasible sets for pipes and compressors in Section 3. The proposed algorithmic framework is presented in Section 4. The numerical results for our computational experiments on various GasLib instances follow in Section 5. Finally, we conclude our paper with further remarks and future research directions in Section 6.

## 2 Problem Formulation

We describe the problem setting in Section 2.1, and explain the gas network modeling along with decision variables and problem parameters in Section 2.2. Finally, we present the MINLP formulation of the problem in Section 2.3.

## 2.1 Problem Setting

In this paper, we consider an isothermal and stationary natural gas network, which is a common industry practice [32]. We denote this network by  $\mathcal{G} = (\mathcal{N}, \mathcal{E})$ , where  $\mathcal{N}$  denotes the set of nodes, and  $\mathcal{E}$  denotes the set of edges. Figure 1 shows an example of a small-scale gas network (taken from [31]). The set  $\mathcal{N}$  consists of the set  $\mathcal{N}_{source}$  of source nodes, the set  $\mathcal{N}_{inner}$  of inner nodes and the set  $\mathcal{N}_{sink}$  of sink nodes. We let  $\mathcal{E} = \mathcal{P} \cup \mathcal{A}$ , where  $\mathcal{P}$  and  $\mathcal{A}$  denote the set of passive and active elements, respectively. In our notation, set  $\mathcal{P}$  consists of the set of pipes, resistors and connections (i.e., short pipes). For simplicity, we refer to the elements of this set as pipes when necessary. We split  $\mathcal{A}$  into the set  $\mathcal{C}$  of compressors, the set  $\mathcal{V}$  of control valves, and the set  $\mathcal{R}$  of regular valves. For each edge  $(i, j) \in \mathcal{E}$ , we assume that the direction of the gas flow is arbitrary, e.g., it is positive if gas flows from node  $i$  to node  $j$ , and negative otherwise. We restrict ourselves to a simplified compressor station, which consists of a bidirectional single compressor unit (i.e., compressor). We assume that all nodes are located horizontally (i.e., arcs are at the same height), and all arcs are cylindrical. For each node  $i \in \mathcal{N}$ , we define  $\Delta^+(i) := \{j \in \mathcal{N} : (i, j) \in \mathcal{A}\}$  as the set of outgoing neighbors and  $\Delta^-(i) := \{j \in \mathcal{N} : (j, i) \in \mathcal{A}\}$  as the incoming neighbors of node  $i$ . Also, we respectively define  $\Delta_{\mathcal{C}}^+(i) = \{j \in \mathcal{N}, (i, j) \in \mathcal{C}\}$  and  $\Delta_{\mathcal{C}}^-(i) = \{j \in \mathcal{N}, (j, i) \in \mathcal{C}\}$  as the sets of outgoing and incoming neighbors of node  $i$ , which are connected to this node via a compressor. We denote the set of gas stores linked to node  $i$  as  $\mathcal{S}(i)$ . Finally, set  $\mathcal{T}$  represents the set of periods within the planning horizon.

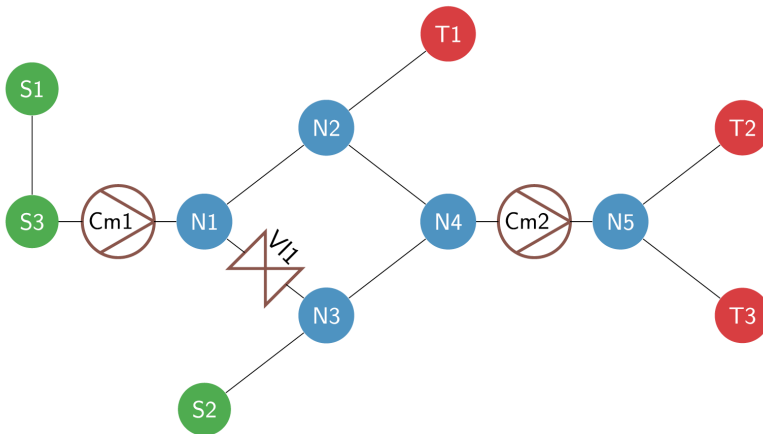


**Fig. 1:** The GasLib-11 instance (figure is taken from [31]). Here,  $\mathcal{N}_{source} = \{S1, S2, S3\}$ ,  $\mathcal{N}_{sink} = \{T1, T2, T3\}$ ,  $\mathcal{N}_{inner} = \{N1, N2, N3, N4, N5\}$ ,  $\mathcal{C} = \{Cm1, Cm2\}$ ,  $\mathcal{R} = \{V11\}$ ,  $\mathcal{P}$  is the set of unlabeled arcs.

## 2.2 Gas Network Modeling

In this section, we explain the physical and operational constraints of network elements. For more detailed explanations on the gas network modeling, we refer the reader to the book [33]. For period  $t \in \mathcal{T}$ , each node  $i \in \mathcal{N}$  is associated with a nonnegative pressure variable  $p_{it}$ . The variable  $p_{it}$  is between lower and upper pressure bounds denoted by  $\underline{p}_i$  and  $\bar{p}_i$ , respectively. Moreover, the gas load parameter at node  $i \in \mathcal{N}$  is denoted by  $q_{it}$  for period  $t \in \mathcal{T}$ . Note that a positive gas load (e.g., supply) is assigned for each  $i \in \mathcal{N}_{source}$  and a negative gas load (e.g., demand) is assigned for each  $i \in \mathcal{N}_{sink}$ . We also let  $q_{it} = 0$  for each  $i \in \mathcal{N}_{inner}$ . We denote the minimum and maximum store levels by  $\underline{s}_j$  and  $\bar{s}_j$ , respectively. For each period  $t \in \mathcal{T}$ , the nonnegative variable  $s_{kt} \in [\underline{s}_k, \bar{s}_k]$  represents the amount of gas (the store level) at store  $k \in \mathcal{S}(i)$  linked to node  $i \in \mathcal{N}$ , whereas the gas injection and withdrawal amounts at store  $k$  with predetermined rates  $\eta_k^+$  and  $\eta_k^-$  are denoted by  $s_{kt}^+$  and  $s_{kt}^-$ , respectively. The gas withdrawals from store  $k$  are associated with a positive supply cost  $C_k^{wd}$ . For each period  $t \in \mathcal{T}$ , the variable  $f_{ijt}$  represents the gas flow through edge  $(i, j) \in \mathcal{E}$ . The flow variable  $f_{ijt}$  is between allowable lower and upper flow limits denoted as  $\underline{f}_{ij}$  and  $\bar{f}_{ij}$ , respectively. For each active element  $(i, j) \in \mathcal{A}$ , we associate a control variable  $x_{ijt} \in \{0, 1\}$ . For each  $(i, j) \in \mathcal{A}$ , the variable  $x_{ijt}$  takes the value 1 if active element  $(i, j)$  is in the operating state, and 0 otherwise. For period  $t \in \mathcal{T}$ , each compressor  $(i, j) \in \mathcal{C}$  is associated with binary start-up and shut-down variables  $u_{ijt}$  and  $v_{ijt}$ , respectively. Whenever compressor  $(i, j)$  is turned on from the off state, the positive start-up cost  $C_{ij}^{up}$  is incurred.

Gas transportation in pipes is governed by the Euler equations, which are a system of hyperbolic partial differential equations (see, e.g., [34]). Finding a solution to this complex system is very hard. Following the common practice, we simplify this system under steady-state conditions to model the pressure losses in pipes

due to internal friction. Under steady-state conditions, gas transportation through each pipe  $(i, j) \in \mathcal{P}$  is governed by the well-known nonlinear and nonconvex Weymouth equation:

$$p_{it}^2 - p_{jt}^2 = w_{ij}|f_{ijt}|f_{ijt} \quad (i, j) \in \mathcal{P}, t \in \mathcal{T}. \quad (1)$$

Here, the resistance coefficient  $w_{ij}$  is often called as the Weymouth coefficient. We note that short pipes are artificial network elements that do not induce pressure losses, i.e.,  $w_{ij} = 0$ . Also, resistors are modeled with relatively small resistance coefficients.

In gas networks, active elements control the gas flow and the pressures of their adjacent nodes. For example, compressors are used to increase the pressure of the incoming gas and transport it over long distances whereas control valves are used to reduce this pressure between its adjacent nodes. For an operating active element, the compression (pressure) ratio  $p_{jt}/p_{it}$  belongs to the interval  $[\underline{a}_{ij}, \bar{a}_{ij}]$  if the direction of the gas flow is positive, and  $p_{it}/p_{jt} \in [\underline{a}_{ij}, \bar{a}_{ij}]$  otherwise. Whenever the active element is closed, nodal pressures at adjacent nodes are decoupled due to blocked gas flow, e.g.,  $f_{ij} = 0$ . We summarize the operational conditions for active elements as follows:

$$x_{ijt} = 0 \implies f_{ijt} = 0 \quad (i, j) \in \mathcal{A}, t \in \mathcal{T} \quad (2a)$$

$$f_{ijt} > 0, x_{ijt} = 1 \implies \frac{p_{jt}}{p_{it}} \in [\underline{a}_{ij}, \bar{a}_{ij}] \quad (i, j) \in \mathcal{A}, t \in \mathcal{T} \quad (2b)$$

$$f_{ijt} < 0, x_{ijt} = 1 \implies \frac{p_{it}}{p_{jt}} \in [\underline{a}_{ij}, \bar{a}_{ij}] \quad (i, j) \in \mathcal{A}, t \in \mathcal{T}. \quad (2c)$$

We assume that gas flows are bidirectional on each active element  $(i, j) \in \mathcal{A}$ , i.e.,  $\underline{f}_{ij} < 0 < \bar{f}_{ij}$ . Also, we let  $1 < \underline{a}_{ij} < \bar{a}_{ij}$  for each compressor  $(i, j) \in \mathcal{C}$ , which results in a pressure increase at node  $i$  (resp. node  $j$ ) in case of a positive (resp. negative) gas flow. Similarly, we have  $0 < \underline{a}_{ij} < \bar{a}_{ij} \leq 1$  for each control valve  $(i, j) \in \mathcal{V}$ . We assume that there is no pressure loss in regular valves, e.g.,  $\underline{a}_{ij} = \bar{a}_{ij} = 1$  for  $(i, j) \in \mathcal{R}$ .

We assume that each compressor  $(i, j) \in \mathcal{C}$  associated with a special type of compressor drive (i.e., gas turbines), which provides the necessary power to compress the gas. Whenever compressor  $(i, j)$  is operating, the turbines consume the gas directly taken from the network as their power source, and the positive fuel consumption cost denoted by  $C_{ij}^{fc}$  is incurred. We denote the fuel consumption (i.e., gas loss) incurred by each compressor  $(i, j)$  with the variable  $l_{ijt}$  for each period  $t \in \mathcal{T}$ . The loss variables depend on the direction of the gas flow, some physical parameter  $H_{ij}$  and isentropic exponent  $\kappa$ . If the gas flows from node  $i$  to node  $j$ , the loss variable depends on the compression ratio  $p_{jt}/p_{it}$ , and  $p_{it}/p_{jt}$  in case of a negative gas flow. We summarize these operational conditions for compressors as follows:

$$x_{ijt} = 0 \implies f_{ijt} = 0, l_{ijt} = 0 \quad (i, j) \in \mathcal{C}, t \in \mathcal{T} \quad (3a)$$

$$f_{ijt} > 0, x_{ijt} = 1 \implies l_{ijt} = H_{ij} \left( \left( \frac{p_{jt}}{p_{it}} \right)^\kappa - 1 \right) f_{ijt} \quad (i, j) \in \mathcal{C}, t \in \mathcal{T} \quad (3b)$$

$$f_{ijt} < 0, x_{ijt} = 1 \implies l_{ijt} = H_{ij} \left( \left( \frac{p_{it}}{p_{jt}} \right)^\kappa - 1 \right) f_{ijt} \quad (i, j) \in \mathcal{C}, t \in \mathcal{T}. \quad (3c)$$

Finally, we consider the switching conditions for each active element  $(i, j) \in \mathcal{A}$ . The minimum up-time restrictions ensure that an active element  $(i, j)$  remains open for at least  $MU_{ij}$  many periods if it is activated. Similarly, the minimum down-time restrictions impose that the network element remains closed for at least  $MD_{ij}$  many periods whenever it is turned down. The start-up and shut-down decisions are also coupled with switching decisions for each compressor  $(i, j) \in \mathcal{C}$ . We summarize the switching conditions for active elements as follows:

$$x_{ijt} - x_{ij(t-1)} \leq x_{ijt'} \quad (i, j) \in \mathcal{A}, t \in \mathcal{T}, t' \in \{t+1, \dots, t+MU_{ij}-1\} \quad (4a)$$

$$x_{ij(t-1)} - x_{ij} \leq 1 - x_{ijt'} \quad (i, j) \in \mathcal{A}, t \in \mathcal{T}, t' \in \{t+1, \dots, t+MD_{ij}-1\} \quad (4b)$$

$$x_{ijt} - x_{ij(t-1)} = u_{ijt} - v_{ijt} \quad (i, j) \in \mathcal{C}, t \in \mathcal{T} \quad (4c)$$

$$u_{ijt} + v_{ijt} \leq 1 \quad (i, j) \in \mathcal{C}, t \in \mathcal{T}. \quad (4d)$$

We note that the switching decisions of compressors are analogous to commitment decisions in the unit commitment problem in power systems (see, e.g., [35]). Finally, we assume that the initial state of each active element is off, i.e., (control) valves are closed and compressors are deactivated.

## 2.3 MINLP Formulation

In this section, we present the MINLP formulation of the multi-period gas transportation and storage problem. Observe that one type of nonlinearity is in the form of  $p_i^2 - p_j^2$  in equation (1). Also, note that these nonnegative pressure variables do not linearly appear elsewhere. Thus, we can easily capture this nonlinearity by introducing a squared pressure (potential) variable  $\pi_{it} \in [\underline{\pi}_i, \bar{\pi}_i]$  for each node  $i \in \mathcal{N}$  and each period  $t \in \mathcal{T}$ , where  $\bar{\pi}_i = \bar{p}_i^2$  and  $\underline{\pi}_i = \underline{p}_i^2$ . This reformulation leads to the following nonconvex equations over two finite intervals:

$$\pi_{it} - \pi_{jt} = w_{ij}|f_{ijt}|f_{ijt} \quad (i, j) \in \mathcal{P}, t \in \mathcal{T} \quad (5a)$$

$$\underline{\alpha}_{ij} \leq f_{ijt} \leq \bar{\alpha}_{ij} \quad (i, j) \in \mathcal{P}, t \in \mathcal{T} \quad (5b)$$

$$\underline{\beta}_{ij} \leq \pi_{it} - \pi_{jt} \leq \bar{\beta}_{ij} \quad (i, j) \in \mathcal{P}, t \in \mathcal{T} \quad (5c)$$

where

$$\begin{aligned} \underline{\alpha}_{ij} &:= \max \left\{ \underline{f}_{ij}, -\sqrt{\frac{\bar{\pi}_j - \underline{\pi}_i}{w_{ij}}} \right\} & \bar{\alpha}_{ij} &:= \min \left\{ \bar{f}_{ij}, \sqrt{\frac{\bar{\pi}_i - \underline{\pi}_j}{w_{ij}}} \right\} \\ \underline{\beta}_{ij} &:= \max \left\{ -w_{ij}(\underline{f}_{ij})^2, \underline{\pi}_i - \bar{\pi}_j \right\} & \bar{\beta}_{ij} &:= \min \left\{ w_{ij}(\bar{f}_{ij})^2, \bar{\pi}_i - \underline{\pi}_j \right\}. \end{aligned}$$

In our gas network modeling, we completely omit nonnegative pressure variables. They can be easily computed (if necessary) once the potential variables are obtained. For each active element  $(i, j) \in \mathcal{A}$ , we let  $\underline{r}_{ij} = (\underline{\alpha}_{ij})^2$ ,  $\bar{r}_{ij} = (\bar{\alpha}_{ij})^2$ , and  $\hat{\kappa} = \kappa/2$  for the fractional exponent used in modeling gas losses induced by compressors.

Now, we are ready to present the mathematical programming formulation of the considered problem with the aforementioned variable and bound changes:

$$\min g(\cdot) \quad (6a)$$

s.t. For each  $t \in \mathcal{T}$ :

$$q_{it} = \sum_{k \in \mathcal{S}(i)} (s_{kt}^+ - s_{kt}^-) + \sum_{k \in \Delta^+(i)} f_{ikt} - \sum_{j \in \Delta^-(i)} f_{jit} + \sum_{j \in \Delta_{\mathcal{C}}^-(i)} l_{ijt} - \sum_{j \in \Delta_{\mathcal{C}}^+(i)} l_{jit} \quad i \in \mathcal{N} \quad (6b)$$

$$s_{kt} = s_{k(t-1)} + \eta_j^+ s_{kt}^+ - \eta_j^- s_{kt}^- \quad i \in \mathcal{N}, k \in \mathcal{S}(i) \quad (6c)$$

$$s_{k|\mathcal{T}|} = s_{k0} \quad i \in \mathcal{N}, k \in \mathcal{S}(i) \quad (6d)$$

$$\underline{\pi}_i \leq \pi_{it} \leq \bar{\pi}_i \quad i \in \mathcal{N} \quad (6e)$$

$$\underline{f}_{ij} \leq f_{ijt} \leq \bar{f}_{ij} \quad (i, j) \in \mathcal{E} \setminus \mathcal{P} \quad (6f)$$

$$f_{ijt} > 0, x_{ijt} = 1 \implies \frac{\pi_{jt}}{\pi_{it}} \in [\underline{r}_{ij}, \bar{r}_{ij}] \quad (i, j) \in \mathcal{A} \quad (6g)$$

$$f_{ijt} < 0, x_{ijt} = 1 \implies \frac{\pi_{it}}{\pi_{jt}} \in [\underline{r}_{ij}, \bar{r}_{ij}] \quad (i, j) \in \mathcal{A} \quad (6h)$$

$$f_{ijt} > 0, x_{ijt} = 1 \implies l_{ijt} = H_{ij} \left( \left( \frac{\pi_{jt}}{\pi_{it}} \right)^{\hat{\kappa}} - 1 \right) f_{ijt} \quad (i, j) \in \mathcal{C} \quad (6i)$$

$$f_{ijt} < 0, x_{ijt} = 1 \implies l_{ijt} = H_{ij} \left( \left( \frac{\pi_{it}}{\pi_{jt}} \right)^{\hat{\kappa}} - 1 \right) f_{ijt} \quad (i, j) \in \mathcal{C} \quad (6j)$$

$$x_{ijt} \in \{0, 1\} \quad (i, j) \in \mathcal{A} \quad (6k)$$

$$u_{ijt}, v_{ijt} \in \{0, 1\} \quad (i, j) \in \mathcal{C} \quad (6l)$$

$$(2a), (3a), (4), (5).$$

In this formulation, the objective function  $g$  in (6a) is some linear objective function, e.g., the total fuel consumption and start-up costs, and the supply cost of gas stores. Constraint (6b) models natural gas flow balance by the conservation of mass at each node. Constraints (6c) and (6d) correspond to the inventory balance equation for the amount of gas stored and the ending storage levels at each store. Constraints (6e) and (6f) are the operational limit constraints for potential and gas flow variables, respectively. Constraints (6g) and (6h) are the operational constraints for the active elements whereas constraints (6i) and (6j) are the fuel consumption equations for compressors. Constraints (6k) and (6l) represent the binary restrictions for control decisions for active arcs, and start-up and shut-down variables for compressors, respectively. We note that problem (6) is (highly) nonlinear and nonconvex due to constraints (5a) and (6g)-(6j).

### 3 Main Results

In this section, we will present our main results. We first introduce the notation used in the remainder of this paper in Section 3.1. We present our convexification results on the feasible set for pipes in Section 3.2, and the feasible set for compressors in Section 3.3. More precisely, we give the convex hull descriptions of these two nonconvex sets and show that they are second-order cone representable (Theorem 1) and power cone representable (Theorem 2), respectively. To compare our convexification approaches, we provide the polyhedral and second-order outer-approximations known from the literature for pipes. We also propose a second-order cone approximation of the feasible set of compressors (Theorem 3) that effectively utilizes the state-of-the-art solvers.

#### 3.1 Notation

For a set  $X \subseteq \mathbb{R}^n$ , we denote the convex hull of  $X$ , the set of extreme points of  $X$  and the interior of  $X$  as  $\text{conv}(X)$ ,  $\text{extr}(X)$  and  $\text{int}(X)$ , respectively. We also denote the projection of  $X$  onto the space of  $x$ -variables as  $\text{proj}_x(X)$ . We define the 3-dimensional power cone parameterized by  $a \in [0, 1]$  as

$$\mathbf{P}_a := \{x \in \mathbb{R}^3 : x_1^a x_2^{1-a} \geq |x_3|, x_1, x_2 \geq 0\}.$$

For a convex set  $Y \subseteq \mathbb{R}^n$ , we say that  $Y$  is conic representable if  $Y = \{x \in \mathbb{R}^n : \exists w \in \mathbb{R}^m : T(x, w) \succeq_K 0\}$  where  $K$  is a proper cone and  $T(\cdot)$  is an affine mapping. In particular, we will call that  $Y$  is polyhedrally representable/SOCr/POWr if  $K$  is a polyhedral/second-order/power cone. Let  $P := \{x \in \mathbb{R}^n : Ax \preceq_K b\}$  be a compact conic representable set and  $z \in \{0, 1\}$ . We will denote the set  $\{x \in \mathbb{R}^n : Ax \preceq_K bz\}$  as  $Pz$ .

Consider a set of the form  $\{(w, x, y) \in \mathbb{R}^3 : w = xy, l_x \leq x \leq u_x, l_y \leq y \leq u_y\}$  with finite variable bounds. We denote the convex hull of this set using McCormick envelopes (see, [36]) as follows:

$$\begin{aligned} \mathcal{M}(l_x, u_x, l_y, u_y) = \{(w, x, y) \in \mathbb{R}^3 : w \geq \max\{l_y x + l_x y - l_x l_y, u_y x + u_x y - u_x u_y\} \\ w \leq \min\{u_y x + l_x y - l_x u_y, l_y x + u_x y - u_x l_y\}\}. \end{aligned}$$

In the remainder of this paper, we omit  $t$  indices for notational brevity. We also drop  $(i, j)$  indices and use them whenever necessary.

#### 3.2 Convexification of the feasible set of a pipe

In this section, we will focus on the feasible set of a specific pipe  $(i, j) \in \mathcal{P}$ , which satisfies the constraints in (5). Assume that gas flow bounds satisfy the relations  $\underline{\alpha}_{ij} \leq 0 \leq \bar{\alpha}_{ij}$  and  $\underline{\beta}_{ij} \leq 0 \leq \bar{\beta}_{ij}$ . We define the following polytope

$$\mathcal{B}_{ij} := \{(f_{ij}, \pi_i, \pi_j) \in \mathbb{R}^3 : \underline{\alpha}_{ij} \leq f_{ij} \leq \bar{\alpha}_{ij}, \underline{\beta}_{ij} \leq \pi_i - \pi_j \leq \bar{\beta}_{ij}, \underline{\pi}_i \leq \pi_i \leq \bar{\pi}_i, \underline{\pi}_j \leq \pi_j \leq \bar{\pi}_j\},$$

and the following (bounded) nonconvex set:

$$\mathcal{X}_{ij} := \{(f_{ij}, \pi_i, \pi_j) \in \mathcal{B}_{ij} : \pi_i - \pi_j = w_{ij} |f_{ij}| f_{ij}\}.$$

We refer to the set  $\mathcal{X}_{ij}$  as the *Weymouth set*, and our aim is to find its convex hull description in this section. It will be convenient to introduce the following sets

$$\mathcal{X}_{ij}^+ := \{(f_{ij}, \pi_i, \pi_j) \in \mathcal{B}_{ij}^+ : \pi_i - \pi_j = w_{ij} f_{ij}^2\} \text{ and } \mathcal{X}_{ij}^- := \{(f_{ij}, \pi_i, \pi_j) \in \mathcal{B}_{ij}^- : \pi_j - \pi_i = w_{ij} f_{ij}^2\},$$

where

$$\begin{aligned} \mathcal{B}_{ij}^+ &:= \{(f_{ij}, \pi_i, \pi_j) \in \mathcal{B}_{ij} : 0 \leq f_{ij} \leq \bar{\alpha}_{ij}, 0 \leq \pi_i - \pi_j \leq \bar{\beta}_{ij}\} \\ \mathcal{B}_{ij}^- &:= \{(f_{ij}, \pi_i, \pi_j) \in \mathcal{B}_{ij} : \underline{\alpha}_{ij} \leq f_{ij} \leq 0, \underline{\beta}_{ij} \leq \pi_i - \pi_j \leq 0\}. \end{aligned}$$

Note that the relation  $\mathcal{X}_{ij} = \mathcal{X}_{ij}^+ \cup \mathcal{X}_{ij}^-$  is trivially satisfied.

##### 3.2.1 Second-order cone representable convex hull

Our first main result is the following theorem, which states that the convex hull of the Weymouth set is SOCr:

**Theorem 1.**  $\text{conv}(\mathcal{X}_{ij})$  is SOCr.

The proof strategy of Theorem 1 is to show that both  $\text{conv}(\mathcal{X}_{ij}^+)$  and  $\text{conv}(\mathcal{X}_{ij}^-)$  are SOCr sets.

**Proposition 1.** We have  $\text{conv}(\mathcal{X}_{ij}^+) = \{(f_{ij}, \pi_i, \pi_j) \in \check{\mathcal{B}}_{ij}^+ : \pi_i - \pi_j \geq w_{ij}f_{ij}^2\}$ , where  $\check{\mathcal{B}}_{ij}^+$  is a polytope. Hence,  $\text{conv}(\mathcal{X}_{ij}^+)$  is SOCr.

*Proof.* Due to [37], we have that

$$\text{conv}(\mathcal{X}_{ij}^+) = \text{conv}(\{(f_{ij}, \pi_i, \pi_j) \in \mathcal{B}_{ij}^+ : \pi_i - \pi_j \geq w_{ij}f_{ij}^2\}) \cap \text{conv}(\{(f_{ij}, \pi_i, \pi_j) \in \mathcal{B}_{ij}^+ : \pi_i - \pi_j \leq w_{ij}f_{ij}^2\}).$$

Notice that the first set is the intersection of the polytope  $\mathcal{B}_{ij}^+$  with the convex quadratic inequality  $\pi_i - \pi_j \geq w_{ij}f_{ij}^2$ , hence, it is already SOCr. The second set is the convex hull of the intersection of the polytope  $\mathcal{B}_{ij}^+$  with the reverse convex constraint  $\pi_i - \pi_j \leq w_{ij}f_{ij}^2$ , which is known to be a polytope due to [38], hence it is also SOCr. Let us denote this polytope by  $\check{\mathcal{B}}_{ij}^+$  which is a subset of  $\mathcal{B}_{ij}^+$ , by construction. Finally, as the intersection of two SOCr sets,  $\text{conv}(\mathcal{X}_{ij}^+)$  is SOCr.  $\square$

We note that the extreme points of the polytope  $\check{\mathcal{B}}_{ij}^+$  can be explicitly identified by a simple procedure (see Algorithm 2 in Appendix A).

The proof of the following proposition is similar to that of Proposition 1, hence, it is omitted.

**Proposition 2.** We have  $\text{conv}(\mathcal{X}_{ij}^-) = \{(f_{ij}, \pi_i, \pi_j) \in \check{\mathcal{B}}_{ij}^- : \pi_j - \pi_i \geq w_{ij}f_{ij}^2\}$ , where  $\check{\mathcal{B}}_{ij}^-$  is a polytope. Hence,  $\text{conv}(\mathcal{X}_{ij}^-)$  is SOCr.

We are now ready to prove Theorem 1.

*Proof of Theorem 1.* Due to Propositions 1 and 2, we deduce that  $\text{conv}(\mathcal{X}_{ij}^+)$  and  $\text{conv}(\mathcal{X}_{ij}^-)$  are SOCr. Since these sets are also compact and satisfy the relation  $\mathcal{X}_{ij} = \mathcal{X}_{ij}^+ \cup \mathcal{X}_{ij}^-$ , the convex hull of their union is also SOCr [39].  $\square$

Since the proof of Theorem 1 is constructive, we are able to give an extended formulation for  $\text{conv}(\mathcal{X}_{ij})$  as below:

$$\text{conv}(\mathcal{X}_{ij}) = \left\{ \begin{array}{l} (f_{ij}, \pi_i, \pi_j) \in \mathbb{R}^3, \\ (f_{ij}^+, \pi_i^+, \pi_j^+) \in \mathbb{R}^3, \\ (f_{ij}^-, \pi_i^-, \pi_j^-) \in \mathbb{R}^3, \\ z_{ij} \in [0, 1] \end{array} : \begin{array}{l} (f_{ij}^+, \pi_i^+, \pi_j^+) \in \check{\mathcal{B}}_{ij}^+ z_{ij}, \quad z_{ij}(\pi_i^+ - \pi_j^+) \geq w_{ij}(f_{ij}^+)^2 \\ (f_{ij}^-, \pi_i^-, \pi_j^-) \in \check{\mathcal{B}}_{ij}^-(1 - z_{ij}), \quad (1 - z_{ij})(\pi_j^- - \pi_i^-) \geq w_{ij}(f_{ij}^-)^2 \\ f_{ij} = f_{ij}^+ + f_{ij}^-, \quad \pi_i = \pi_i^+ + \pi_i^-, \quad \pi_j = \pi_j^+ + \pi_j^- \end{array} \right\}.$$

Here, when we have the binary variable  $z_{ij} = 1$ , the flow is positive and the variables  $(f_{ij}^+, \pi_i^+, \pi_j^+)$  belong to the set  $\check{\mathcal{B}}_{ij}^+$  while the variables  $(f_{ij}^-, \pi_i^-, \pi_j^-)$  are all zero (the case with  $z_{ij} = 0$  is exactly the opposite). Although the above extended formulation gives the convex hull of the Weymouth set for a specific pipe, hence, the variable  $z_{ij}$  can be relaxed to a continuous variable, we need to enforce it to take a binary value in the gas network optimization problems.

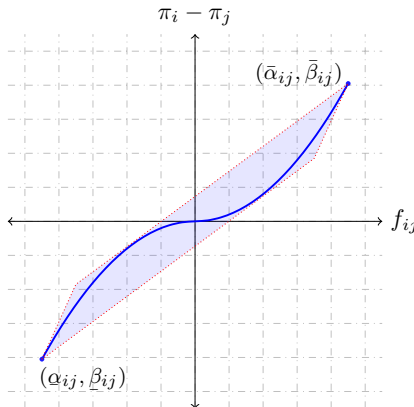


**Fig. 2:** Polyhedral outer-approximation of  $\mathcal{X}_{ij}$  in the  $(f_{ij}, \pi_i - \pi_j)$ -space.

### 3.2.2 Outer-approximations via different convex sets

Here, we introduce two convex outer-approximations of the Weymouth set taken from the literature that involve polyhedrally representable and SOCr sets.

#### *Polyhedral outer-approximation*

We now provide a polyhedral approximation of the Weymouth set, which is adapted from [12]. We use four hyperplanes to obtain the polyhedrally representable outer-approximation of this set. Our construction is geometrically illustrated in Figure 2 in the space of  $(f_{ij}, \pi_i - \pi_j)$ -variables. To be precise, we first find the line passing through  $(\underline{\alpha}_{ij}, \underline{\beta}_{ij})$  and tangent to the curve at point  $(a_{ij}, w_{ij}a_{ij}^2)$  with  $f_{ij}, \pi_i - \pi_j \geq 0$ , where  $a_{ij}$  is some constant. Similarly, we obtain the line passing through  $(\bar{\alpha}_{ij}, \bar{\beta}_{ij})$  and tangent to this curve at point  $(a_{ij}, -w_{ij}a_{ij}^2)$  with  $f_{ij}, \pi_i - \pi_j \leq 0$ . For the remaining hyperplanes, we find two tangent lines to this curve at the points  $(\underline{\alpha}_{ij}, \underline{\beta}_{ij})$  and  $(\bar{\alpha}_{ij}, \bar{\beta}_{ij})$ , respectively. After some simple calculations, the polyhedral outer-approximation of the Weymouth set is formed by the set

$$\mathcal{X}_{\text{poly}} := \{(f_{ij}, \pi_i, \pi_j) \in \mathbb{R}^3 : \pi_i - \pi_j \geq w_{ij}a_{ij}(2f_{ij} - a_{ij}), \pi_i - \pi_j \leq w_{ij}b_{ij}(b_{ij} - 2f_{ij}) \\ \pi_i - \pi_j \geq w_{ij}\bar{\alpha}_{ij}(2f_{ij} - \bar{\alpha}_{ij}), \pi_i - \pi_j \leq w_{ij}\underline{\alpha}_{ij}(\underline{\alpha}_{ij} - 2f_{ij})\},$$

where  $a_{ij} = (1 - \sqrt{2})\underline{\alpha}_{ij}$  and  $b_{ij} = (1 - \sqrt{2})\bar{\alpha}_{ij}$ .

Note that other polyhedral outer-approximations of the Weymouth set such as piecewise linearizations (see, e.g., [12]) can also be applied. However, these formulations require using many binary variables for high-resolution solutions, even for a small-scale network. In this case, the global solver might fail to provide even locally optimal solutions as the size of the gas network increases due to the time limit.

#### *Second-order cone outer-approximation*

A known SOCr relaxation of the Weymouth set is defined as follows [20] and used in the context of the gas expansion planning problem:

$$\mathcal{X}_{\text{socr}} := \{(f_{ij}, \pi_i, \pi_j) \in \mathbb{R}^3 : \exists(\pi', z) \in \mathbb{R} \times [0, 1] : \underline{\alpha}_{ij}(1 - z_{ij}) \leq f_{ij} \leq \bar{\alpha}_{ij}z_{ij}, \underline{\beta}_{ij}(1 - z_{ij}) \leq \pi_i - \pi_j \leq \bar{\beta}_{ij}z_{ij} \\ \pi'_{ij} \geq w_{ij}f_{ij}^2, (\pi'_{ij}, 2z_{ij} - 1, \pi_i - \pi_j) \in \mathcal{M}(-1, 1, \underline{\beta}_{ij}, \bar{\beta}_{ij})\}.$$

Note that this set involves a second-order cone constraints and McCormick inequalities, but does not give the convex hull in general.

**Remark 1.** We note that in some GasLib test instances, flow directions are known to be positive. In such cases, the polyhedral and second-order cone outer-approximations can be formed by the sets  $\mathcal{X}_{\text{poly}}^+ := \{(f_{ij}, \pi_i, \pi_j) \in \mathcal{B}_{ij}^+ : \pi_i - \pi_j \leq \frac{\bar{\beta}_{ij}}{\underline{\alpha}_{ij}}f_{ij}\}$  and  $\mathcal{X}_{\text{socr}}^+ := \{(f_{ij}, \pi_i, \pi_j) \in \check{\mathcal{B}}_{ij}^+ : \pi_i - \pi_j \geq w_{ij}f_{ij}^2\}$ , respectively. In our computational study, we will use these sets for the cases with positive gas flows. We also note that the set  $\mathcal{X}_{\text{socr}}$  leads to the convex hull of the Weymouth set in case of positive flows. Similar results also follow for both sets when the flow directions are negative.

### 3.3 Convexification of the feasible set of a compressor

In this section, we will focus on the feasible set of a specific compressor  $(i, j) \in \mathcal{C}$ , which satisfies the constraints in (6e)-(6k). We define the following polytopes with  $1 < r_{ij} < \bar{r}_{ij}$ :

$$\Pi_{ij} := \left\{ (\pi_i, \pi_j) \in [\underline{\pi}_i, \bar{\pi}_i] \times [\underline{\pi}_j, \bar{\pi}_j] : r_{ij} \leq \frac{\pi_j}{\pi_i} \leq \bar{r}_{ij} \right\}, \quad \Pi_{ji} := \left\{ (\pi_i, \pi_j) \in [\underline{\pi}_i, \bar{\pi}_i] \times [\underline{\pi}_j, \bar{\pi}_j] : r_{ij} \leq \frac{\pi_i}{\pi_j} \leq \bar{r}_{ij} \right\},$$

and the (bounded) nonconvex set  $\mathcal{L}_{ij} := \mathcal{L}_{ij}^+ \cup \mathcal{L}_{ij}^- \cup \mathcal{L}_{ij}^0$ , where

$$\mathcal{L}_{ij}^+ := \{(\pi_i, \pi_j, f_{ij}, l_{ij}, x_{ij}) \in \mathbb{R}^4 \times \{1\} : l_{ij} = H_{ij}((\pi_j/\pi_i)^{\hat{\kappa}} - 1)f_{ij}, (\pi_i, \pi_j) \in \Pi_{ij}, f_{ij} \in [0, \bar{f}_{ij}]\} \\ \mathcal{L}_{ij}^- := \{(\pi_i, \pi_j, f_{ij}, l_{ij}, x_{ij}) \in \mathbb{R}^4 \times \{1\} : l_{ij} = H_{ij}((\pi_i/\pi_j)^{\hat{\kappa}} - 1)f_{ij}, (\pi_i, \pi_j) \in \Pi_{ji}, f_{ij} \in [\underline{f}_{ij}, 0]\} \\ \mathcal{L}_{ij}^0 := \{(\pi_i, \pi_j, f_{ij}, l_{ij}, x_{ij}) \in \mathbb{R}^2 \times \{0\}^3 : \underline{\pi}_i \leq \pi_i \leq \bar{\pi}_i, \underline{\pi}_j \leq \pi_j \leq \bar{\pi}_j\}.$$

We refer to the set  $\mathcal{L}_{ij}$  as the *compression set*, and our aim is to find its convex hull description in this section.

### 3.3.1 Power cone representable convex hull

We state our second main result in the following theorem:

**Theorem 2.**  $\text{conv}(\mathcal{L}_{ij})$  is POWr.

The proof strategy of Theorem 2 is to show that the convex hull of extreme points of the sets  $\mathcal{L}_{ij}^+$ ,  $\mathcal{L}_{ij}^-$  and  $\mathcal{L}_{ij}^0$  are POWr sets. The polytope  $\mathcal{L}_{ij}^0$  is trivially POWr. Hence, we will only focus on  $\mathcal{L}_{ij}^+$  and  $\mathcal{L}_{ij}^-$ .

Next, we present a series of preliminary results that will be used in the proof that will eventually give a complete extreme point characterization of the set  $\mathcal{L}_{ij}^+$  in Proposition 3.

**Lemma 1.** Let  $(\pi_i, \pi_j, f_{ij}, l_{ij}, x_{ij}) \in \text{extr}(\mathcal{L}_{ij}^+)$ . Then,

- (i)  $f_{ij} \in \{0, \bar{f}_{ij}\}$ .
- (ii)  $(\pi_i, \pi_j) \notin \text{int}(\Pi_{ij})$ .
- (iii) Either  $\pi_i \in \{\underline{\pi}_i, \bar{\pi}_i\}$  or  $\pi_j \in \{\underline{\pi}_j, \bar{\pi}_j\}$ .

*Proof.*

- (i) Suppose that there exists a point  $y = (\pi_i, \pi_j, f_{ij}, l_{ij}, x_{ij}) \in \text{extr}(\mathcal{L}_{ij}^+)$  with  $0 < f_{ij} < \bar{f}_{ij}$ . Then, there exists a small enough  $\epsilon > 0$  such that  $y' = (\pi_i, \pi_j, (1 + \epsilon)f_{ij}, (1 + \epsilon)l_{ij}, x_{ij}) \in \mathcal{L}_{ij}^+$  and  $y'' = (\pi_i, \pi_j, (1 - \epsilon)f_{ij}, (1 - \epsilon)l_{ij}, x_{ij}) \in \mathcal{L}_{ij}^+$ . This implies that  $y \notin \text{extr}(\mathcal{L}_{ij}^+)$  since  $y = \frac{1}{2}y' + \frac{1}{2}y''$ , which leads to a contradiction.
- (ii) We first show that  $(\pi_i, \pi_j) \notin \text{int}(\Pi_{ij})$ . In fact, suppose that there exists a point  $y = (\pi_i, \pi_j, f_{ij}, l_{ij}, x_{ij}) \in \text{extr}(\mathcal{L}_{ij}^+)$  with  $(\pi_i, \pi_j) \in \text{int}(\Pi_{ij})$ . Then, there exists a small enough  $\epsilon > 0$  such that  $y' = ((1 + \epsilon)\pi_i, (1 + \epsilon)\pi_j, f_{ij}, l_{ij}, x_{ij}) \in \mathcal{L}_{ij}^+$  and  $y'' = ((1 - \epsilon)\pi_i, (1 - \epsilon)\pi_j, f_{ij}, l_{ij}, x_{ij}) \in \mathcal{L}_{ij}^+$ . This implies that  $y = \frac{1}{2}y' + \frac{1}{2}y''$ , which leads to a contradiction.
- (iii) Suppose that there exists a point  $y = (\pi_i, \pi_j, f_{ij}, l_{ij}, x_{ij}) \in \text{extr}(\mathcal{L}_{ij}^+)$  with  $\underline{\pi}_i < \pi_i < \bar{\pi}_i$  and  $\underline{\pi}_j < \pi_j < \bar{\pi}_j$ . Due to Part (ii), we must have  $\frac{\pi_i}{\pi_j} \in \{r_{ij}, \bar{r}_{ij}\}$ . The rest of the proof is the same as the proof of Part (ii). □

Using Lemma 1, we now present the following proposition on the characterization of the extreme points of the nonconvex set  $\mathcal{L}_{ij}^+$ .

**Proposition 3.**  $\text{extr}(\mathcal{L}_{ij}^+)$  is contained in  $\mathcal{U}_{ij}^{+1} \cup \mathcal{U}_{ij}^{+2} \cup \mathcal{U}_{ij}^{+3} \cup \mathcal{U}_{ij}^{+4} \cup \mathcal{U}_{ij}^{+5}$  where

$$\begin{aligned} \mathcal{U}_{ij}^{+1} &:= \{(\pi_i, \pi_j, 0, 0, 1) \in \mathbb{R}^5 : (\pi_i, \pi_j) \in \Pi_{ij}\} \\ \mathcal{U}_{ij}^{+2} &:= \{(\underline{\pi}_i, \pi_j, \bar{f}_{ij}, l_{ij}, 1) \in \mathbb{R}^5 : l_{ij} = H_{ij}\bar{f}_{ij}((\pi_j/\underline{\pi}_i)^{\hat{\kappa}} - 1), \max\{\underline{\pi}_j, \underline{\pi}_i r_{ij}\} \leq \pi_j \leq \min\{\bar{\pi}_j, \underline{\pi}_i \bar{r}_{ij}\}\} \\ \mathcal{U}_{ij}^{+3} &:= \{(\bar{\pi}_i, \pi_j, \bar{f}_{ij}, l_{ij}, 1) \in \mathbb{R}^5 : l_{ij} = H_{ij}\bar{f}_{ij}((\pi_j/\bar{\pi}_i)^{\hat{\kappa}} - 1), \max\{\underline{\pi}_j, \bar{\pi}_i r_{ij}\} \leq \pi_j \leq \min\{\bar{\pi}_j, \bar{\pi}_i \bar{r}_{ij}\}\} \\ \mathcal{U}_{ij}^{+4} &:= \{(\pi_i, \underline{\pi}_j, \bar{f}_{ij}, l_{ij}, 1) \in \mathbb{R}^5 : l_{ij} = H_{ij}\bar{f}_{ij}((\pi_j/\pi_i)^{\hat{\kappa}} - 1), \max\{\underline{\pi}_i, \underline{\pi}_j/\bar{r}_{ij}\} \leq \pi_i \leq \min\{\bar{\pi}_i, \underline{\pi}_j/r_{ij}\}\} \\ \mathcal{U}_{ij}^{+5} &:= \{(\pi_i, \bar{\pi}_j, \bar{f}_{ij}, l_{ij}, 1) \in \mathbb{R}^5 : l_{ij} = H_{ij}\bar{f}_{ij}((\pi_j/\pi_i)^{\hat{\kappa}} - 1), \max\{\underline{\pi}_i, \bar{\pi}_j/\bar{r}_{ij}\} \leq \pi_i \leq \min\{\bar{\pi}_i, \bar{\pi}_j/r_{ij}\}\}. \end{aligned}$$

The following lemma follows from the fact that for  $n \in (0, 1)$ ,  $u \leq x^n$  is equivalent to  $(x, 1, u) \in \mathbf{P}_n$  over  $(u, x) \in \mathbb{R}_+^2$ .

**Lemma 2.** Consider the following nonconvex set

$$\mathcal{V}^n(a, b, \underline{x}, \bar{x}) = \{(x, y) \in \mathbb{R}_+^2 : y = a((x/b)^n - 1), \underline{x} \leq x \leq \bar{x}\},$$

where  $n \in (0, 1)$ ,  $a > 0$  and  $0 < b \leq \underline{x} \leq \bar{x}$ . Then,

$$\begin{aligned} \text{conv}(\mathcal{V}^n(a, b, \underline{x}, \bar{x})) &= \{(x, y) \in \mathbb{R}_+^2 : \exists u \in \mathbb{R}_+ : (x/b, 1, u) \in \mathbf{P}_n, y = a(u - 1), \\ &\quad y \geq a\left(\frac{(\bar{x}/b)^n - (\underline{x}/b)^n}{\bar{x} - \underline{x}}\right)(x - \underline{x}) + a((\underline{x}/b)^n - 1)\}, \end{aligned}$$

is POWr.

The following lemma follows from the fact that for  $n \in (0, 1)$ ,  $u \geq x^{-n}$  is equivalent to  $(u, x, 1) \in \mathbf{P}_{\frac{1}{1+n}}$  over  $(u, x) \in \mathbb{R}_{++}^2$ .

**Lemma 3.** Consider the following nonconvex set

$$\mathcal{W}^n(a, b, \underline{x}, \bar{x}) = \{(x, y) \in \mathbb{R}_+^2 : y = a((b/x)^n - 1), \underline{x} \leq x \leq \bar{x}\},$$

where  $n \in (0, 1)$ ,  $a > 0$  and  $0 \leq \underline{x} \leq \bar{x} < b$ . Then,

$$\begin{aligned} \text{conv}(\mathcal{W}^n(a, b, \underline{x}, \bar{x})) &= \{(x, y) \in \mathbb{R}_+^2 : \exists u \in \mathbb{R}_+ : (u, x/b, 1) \in \mathbf{P}_{\frac{1}{1+n}}, y = a(u - 1), \\ &\quad y \leq a\left(\frac{(b/\bar{x})^n - (b/\underline{x})^n}{\bar{x} - \underline{x}}\right)(x - \underline{x}) + a((b/\underline{x})^n - 1)\}, \end{aligned}$$

is POWr.

The following proposition is an immediate consequence of Proposition 3, Lemma 2 and Lemma 3:

**Proposition 4.** *We have*

$$\begin{aligned} \text{conv}(\mathcal{U}_{ij}^{+2}) &= \{(\underline{\pi}_i, \pi_j, \bar{f}_{ij}, l_{ij}, 1) \in \mathbb{R}^5 : (\pi_i, l_{ij}) \in \text{conv}(\mathcal{V}^{\hat{\kappa}}(H_{ij}\bar{f}_{ij}, \underline{\pi}_i, \max\{\underline{\pi}_j, \underline{\pi}_i r_{ij}\}, \min\{\bar{\pi}_j, \underline{\pi}_i \bar{r}_{ij}\}))\} \\ \text{conv}(\mathcal{U}_{ij}^{+3}) &= \{(\bar{\pi}_i, \pi_j, \bar{f}_{ij}, l_{ij}, 1) \in \mathbb{R}^5 : (\pi_i, l_{ij}) \in \text{conv}(\mathcal{V}^{\hat{\kappa}}(H_{ij}\bar{f}_{ij}, \bar{\pi}_i, \max\{\underline{\pi}_j, \bar{\pi}_i r_{ij}\}, \min\{\bar{\pi}_j, \bar{\pi}_i \bar{r}_{ij}\}))\} \\ \text{conv}(\mathcal{U}_{ij}^{+4}) &= \{(\pi_i, \underline{\pi}_j, \bar{f}_{ij}, l_{ij}, 1) \in \mathbb{R}^5 : (\pi_j, l_{ij}) \in \text{conv}(\mathcal{W}^{\hat{\kappa}}(H_{ij}\bar{f}_{ij}, \underline{\pi}_j, \max\{\underline{\pi}_i, \underline{\pi}_j/\bar{r}_{ij}\}, \min\{\bar{\pi}_i, \underline{\pi}_j/r_{ij}\}))\} \\ \text{conv}(\mathcal{U}_{ij}^{+5}) &= \{(\pi_i, \bar{\pi}_j, \bar{f}_{ij}, l_{ij}, 1) \in \mathbb{R}^5 : (\pi_j, l_{ij}) \in \text{conv}(\mathcal{W}^{\hat{\kappa}}(H_{ij}\bar{f}_{ij}, \bar{\pi}_j, \max\{\underline{\pi}_i, \bar{\pi}_j/\bar{r}_{ij}\}, \min\{\bar{\pi}_i, \bar{\pi}_j/r_{ij}\}))\}. \end{aligned}$$

**Proposition 5.**  $\text{conv}(\mathcal{L}_{ij}^+)$  is POWr.

*Proof.* Recall that we have  $\text{extr}(\mathcal{L}_{ij}^+) \subseteq \mathcal{U}_{ij}^{+1} \cup \mathcal{U}_{ij}^{+2} \cup \mathcal{U}_{ij}^{+3} \cup \mathcal{U}_{ij}^{+4} \cup \mathcal{U}_{ij}^{+5} \subseteq \mathcal{L}_{ij}^+$ . Being a polytope,  $\mathcal{U}_{ij}^1$  is trivially POWr. On the other hand,  $\text{conv}(\mathcal{U}_{ij}^{+2}), \dots, \text{conv}(\mathcal{U}_{ij}^{+5})$  are POWr sets due to Proposition 4. Since  $\text{conv}(\mathcal{U}_{ij}^{+1}), \dots, \text{conv}(\mathcal{U}_{ij}^{+5})$  are compact POWr sets and the set  $\text{conv}(\mathcal{L}_{ij}^+)$  is the convex hull of their union, the results follows due to [39].  $\square$

Let us present a similar analysis for the extreme point characterization of the set  $\mathcal{L}_{ij}^-$ . The proof is omitted since they are similar to that of Lemma 1.

**Lemma 4.** *Let  $(\pi_i, \pi_j, f_{ij}, l_{ij}, x_{ij}) \in \text{extr}(\mathcal{L}_{ij}^-)$ . Then,*

- (i)  $f_{ij} \in \{\underline{f}_{ij}, 0\}$ .
- (ii) *Either*  $\pi_i \in \{\underline{\pi}_i, \bar{\pi}_i\}$  *or*  $\pi_j \in \{\underline{\pi}_j, \bar{\pi}_j\}$ .

Using Lemma 4, we now present the following proposition on the characterization of the extreme points of the nonconvex set  $\mathcal{L}_{ij}^-$ .

**Proposition 6.**  $\text{extr}(\mathcal{L}_{ij}^-)$  is contained in  $\mathcal{U}_{ij}^{-1} \cup \mathcal{U}_{ij}^{-2} \cup \mathcal{U}_{ij}^{-3} \cup \mathcal{U}_{ij}^{-4} \cup \mathcal{U}_{ij}^{-5}$  where

$$\begin{aligned} \mathcal{U}_{ij}^{-1} &:= \{(\pi_i, \pi_j, 0, 0, 1) \in \mathbb{R}^5 : (\pi_i, \pi_j) \in \Pi_{ji}\} \\ \mathcal{U}_{ij}^{-2} &:= \{(\pi_i, \underline{\pi}_j, \underline{f}_{ij}, l_{ij}, 1) \in \mathbb{R}^5 : l_{ij} = H_{ij}\underline{f}_{ij}((\pi_i/\underline{\pi}_j)^{\hat{\kappa}} - 1), \max\{\underline{\pi}_i, \underline{\pi}_j r_{ij}\} \leq \pi_i \leq \min\{\bar{\pi}_i, \underline{\pi}_j \bar{r}_{ij}\}\} \\ \mathcal{U}_{ij}^{-3} &:= \{(\pi_i, \bar{\pi}_j, \underline{f}_{ij}, l_{ij}, 1) \in \mathbb{R}^5 : l_{ij} = H_{ij}\underline{f}_{ij}((\pi_i/\bar{\pi}_j)^{\hat{\kappa}} - 1), \max\{\underline{\pi}_i, \bar{\pi}_j r_{ij}\} \leq \pi_i \leq \min\{\bar{\pi}_i, \bar{\pi}_j \bar{r}_{ij}\}\} \\ \mathcal{U}_{ij}^{-4} &:= \{(\underline{\pi}_i, \pi_j, \underline{f}_{ij}, l_{ij}, 1) \in \mathbb{R}^5 : l_{ij} = H_{ij}\underline{f}_{ij}((\underline{\pi}_i/\pi_j)^{\hat{\kappa}} - 1), \max\{\underline{\pi}_j, \underline{\pi}_i/\bar{r}_{ij}\} \leq \pi_j \leq \min\{\bar{\pi}_j, \underline{\pi}_i/r_{ij}\}\} \\ \mathcal{U}_{ij}^{-5} &:= \{(\bar{\pi}_i, \pi_j, \underline{f}_{ij}, l_{ij}, 1) \in \mathbb{R}^5 : l_{ij} = H_{ij}\underline{f}_{ij}((\bar{\pi}_i/\pi_j)^{\hat{\kappa}} - 1), \max\{\underline{\pi}_j, \bar{\pi}_i/\bar{r}_{ij}\} \leq \pi_j \leq \min\{\bar{\pi}_j, \bar{\pi}_i/r_{ij}\}\}. \end{aligned}$$

The following proposition is an immediate consequence of Proposition 6, Lemma 2 and Lemma 3:

**Proposition 7.** *We have*

$$\begin{aligned} \text{conv}(\mathcal{U}_{ij}^{-2}) &= \{(\pi_i, \underline{\pi}_j, \underline{f}_{ij}, l_{ij}, 1) \in \mathbb{R}^5 : (\pi_i, -l_{ij}) \in \text{conv}(\mathcal{V}^{\hat{\kappa}}(-H_{ij}\underline{f}_{ij}, \underline{\pi}_j, \max\{\underline{\pi}_i, \underline{\pi}_j r_{ij}\}, \min\{\bar{\pi}_i, \underline{\pi}_j \bar{r}_{ij}\}))\} \\ \text{conv}(\mathcal{U}_{ij}^{-3}) &= \{(\pi_i, \bar{\pi}_j, \underline{f}_{ij}, l_{ij}, 1) \in \mathbb{R}^5 : (\pi_i, -l_{ij}) \in \text{conv}(\mathcal{V}^{\hat{\kappa}}(-H_{ij}\underline{f}_{ij}, \bar{\pi}_j, \max\{\underline{\pi}_i, \bar{\pi}_j r_{ij}\}, \min\{\bar{\pi}_i, \bar{\pi}_j \bar{r}_{ij}\}))\} \\ \text{conv}(\mathcal{U}_{ij}^{-4}) &= \{(\underline{\pi}_i, \pi_j, \underline{f}_{ij}, l_{ij}, 1) \in \mathbb{R}^5 : (\pi_j, -l_{ij}) \in \text{conv}(\mathcal{W}^{\hat{\kappa}}(-H_{ij}\underline{f}_{ij}, \underline{\pi}_i, \max\{\underline{\pi}_j, \underline{\pi}_i/\bar{r}_{ij}\}, \min\{\bar{\pi}_j, \underline{\pi}_i/r_{ij}\}))\} \\ \text{conv}(\mathcal{U}_{ij}^{-5}) &= \{(\bar{\pi}_i, \pi_j, \underline{f}_{ij}, l_{ij}, 1) \in \mathbb{R}^5 : (\pi_j, -l_{ij}) \in \text{conv}(\mathcal{W}^{\hat{\kappa}}(-H_{ij}\underline{f}_{ij}, \bar{\pi}_i, \max\{\underline{\pi}_j, \bar{\pi}_i/\bar{r}_{ij}\}, \min\{\bar{\pi}_j, \bar{\pi}_i/r_{ij}\}))\}. \end{aligned}$$

**Proposition 8.**  $\text{conv}(\mathcal{L}_{ij}^-)$  and  $\text{conv}(\mathcal{L}_{ij}^0)$  are POWr.

We are now ready to prove Theorem 2.

*Proof of Theorem 2.* Due to Propositions 5 and 8, we deduce that  $\text{conv}(\mathcal{L}_{ij}^+)$ ,  $\text{conv}(\mathcal{L}_{ij}^-)$  and  $\text{conv}(\mathcal{L}_{ij}^0)$  are POWr. Since these sets are also compact and satisfy the relation  $\mathcal{L}_{ij} = \mathcal{L}_{ij}^+ \cup \mathcal{L}_{ij}^- \cup \mathcal{L}_{ij}^0$ , the convex hull of their union is also POWr [39].  $\square$

We note that although conic interior solvers allow for non-symmetric cones, e.g., power cones, their algorithmic frameworks are not efficient in solving MINLPs with non-symmetric cones. On the other hand, MISOCPs can be solved quite efficiently at the state-of-the-art, see, e.g., Mittelmann benchmarks [40]. To fully utilize the current solvers, we propose an SOCr outer-approximation of the compression set below.

### 3.3.2 Second-order cone representable outer-approximation

Here, we provide an outer-approximation to the power cone representable convex hull of  $\mathcal{L}_{ij}$  for practical application. For this purpose, we particularly focus on the isentropic exponent  $\kappa$ . In practice, this physical parameter can be approximated by the constant 0.228 [33]. In this paper, we will also follow the common practice and set the exponent  $\hat{\kappa} = \kappa/2$  to 0.114. Our task is then reduced to finding an outer-approximation to the nontrivial POWr sets, in particular, finding an outer-approximation to  $\mathcal{V}^{\hat{\kappa}}(a, b, \underline{x}, \bar{x})$  and  $\mathcal{W}^{\hat{\kappa}}(a, b, \underline{x}, \bar{x})$  in Propositions 4 and 7. For that, we focus a very special case and overestimate  $\hat{\kappa}$  by the constant 0.125. The following lemmas formalize this case.

**Lemma 5.** Consider the following convex set

$$\begin{aligned} \hat{\mathcal{V}}(a, b, \underline{x}, \bar{x}) = \{ & (x, y) \in \mathbb{R}_+^2 : \exists u \in \mathbb{R}_+ : u \leq x^{1/8}, y = a(u - 1), \underline{x} \leq x \leq \bar{x} \\ & y \geq a \left( \frac{(\bar{x}/b)^n - (x/b)^n}{\bar{x} - x} \right) (x - \underline{x}) + a((x/b)^n - 1) \}, \end{aligned}$$

where  $n = 0.114$ ,  $a > 0$  and  $0 < b \leq \underline{x} \leq \bar{x}$ . Then,  $\hat{\mathcal{V}}(a, b, \underline{x}, \bar{x})$  is SOCr. Moreover, it provides an outer-approximation to  $\text{conv}(\mathcal{V}^n(a, b, \underline{x}, \bar{x}))$ .

*Proof.* Suppose  $n = 0.114$ . Then, the proof immediately follows from the following relation

$$\begin{aligned} \{(u, x) \in \mathbb{R}_+^2 : u \leq x^n\} & \subseteq \{(u, x) \in \mathbb{R}_+^2 : u \leq x^{1/8}\} \\ & = \{(u, x) \in \mathbb{R}_+^2 : \exists v \in \mathbb{R}_+^2 : u^2 \leq v_1, v_1^2 \leq v_2, v_2^2 \leq x\}. \end{aligned}$$

□

**Lemma 6.** Consider the following convex set

$$\begin{aligned} \hat{\mathcal{W}}(a, b, \underline{x}, \bar{x}) = \{ & (x, y) \in \mathbb{R}_+^2 : \exists u \in \mathbb{R}_+ : u \geq x^{-1/9}, y = a(u - 1), \underline{x} \leq x \leq \bar{x} \\ & y \leq a \left( \frac{(b/\bar{x})^n - (b/x)^n}{\bar{x} - x} \right) (x - \underline{x}) + a((b/x)^n - 1) \}, \end{aligned}$$

where  $n = 0.114$ ,  $a > 0$  and  $0 \leq \underline{x} \leq \bar{x} < b$ . Then,  $\hat{\mathcal{W}}(a, b, \underline{x}, \bar{x})$  is SOCr. Moreover, it provides an outer-approximation to  $\text{conv}(\mathcal{W}^n(a, b, \underline{x}, \bar{x}))$ .

*Proof.* Suppose  $n = 0.114$ . Then, the proof immediately follows from the following relation

$$\begin{aligned} \{(u, x) \in \mathbb{R}_{++}^2 : u \geq x^{-n}\} & \subseteq \{(u, x) \in \mathbb{R}_{++}^2 : u \geq x^{-1/9}\} \\ & = \{(u, x) \in \mathbb{R}_{++}^2 : \exists v \in \mathbb{R}_+^3 : uv_1 \geq 1, v_2 \geq v_1^2, v_3 \geq v_2^2, ux \geq v_3^2\}. \end{aligned}$$

□

The following proposition is an immediate consequence of Proposition 4, Lemma 5 and Lemma 6:

**Proposition 9.**  $\text{conv}(\mathcal{L}_{ij}^+)$  is contained in  $\hat{\mathcal{L}}_{ij}^+ := \hat{\mathcal{U}}_{ij}^{+1} \cup \hat{\mathcal{U}}_{ij}^{+2} \cup \hat{\mathcal{U}}_{ij}^{+3} \cup \hat{\mathcal{U}}_{ij}^{+4} \cup \hat{\mathcal{U}}_{ij}^{+5}$  where

$$\begin{aligned} \hat{\mathcal{U}}_{ij}^{+2} & = \{(\pi_i, \pi_j, \bar{f}_{ij}, l_{ij}, 1) \in \mathbb{R}^5 : (\pi_i, l_{ij}) \in \hat{\mathcal{V}}(H_{ij}\bar{f}_{ij}, \pi_i, \max\{\underline{\pi}_j, \pi_i r_{ij}\}, \min\{\bar{\pi}_j, \pi_i \bar{r}_{ij}\})\} \\ \hat{\mathcal{U}}_{ij}^{+3} & = \{(\bar{\pi}_i, \pi_j, \bar{f}_{ij}, l_{ij}, 1) \in \mathbb{R}^5 : (\pi_i, l_{ij}) \in \hat{\mathcal{V}}(H_{ij}\bar{f}_{ij}, \bar{\pi}_i, \max\{\underline{\pi}_j, \bar{\pi}_i r_{ij}\}, \min\{\bar{\pi}_j, \bar{\pi}_i \bar{r}_{ij}\})\} \\ \hat{\mathcal{U}}_{ij}^{+4} & = \{(\pi_i, \underline{\pi}_j, \bar{f}_{ij}, l_{ij}, 1) \in \mathbb{R}^5 : (\pi_j, l_{ij}) \in \hat{\mathcal{W}}(H_{ij}\bar{f}_{ij}, \underline{\pi}_j, \max\{\underline{\pi}_i, \underline{\pi}_j/\bar{r}_{ij}\}, \min\{\bar{\pi}_i, \underline{\pi}_j/r_{ij}\})\} \\ \hat{\mathcal{U}}_{ij}^{+5} & = \{(\pi_i, \bar{\pi}_j, \bar{f}_{ij}, l_{ij}, 1) \in \mathbb{R}^5 : (\pi_j, l_{ij}) \in \hat{\mathcal{W}}(H_{ij}\bar{f}_{ij}, \bar{\pi}_j, \max\{\underline{\pi}_i, \bar{\pi}_j/\bar{r}_{ij}\}, \min\{\bar{\pi}_i, \bar{\pi}_j/r_{ij}\})\}. \end{aligned}$$

Moreover,  $\text{conv}(\hat{\mathcal{L}}_{ij}^+)$  is SOCr.

Similarly, the following proposition is an immediate consequence of Proposition 7, Lemma 5 and Lemma 6:

**Proposition 10.**  $\text{conv}(\mathcal{L}_{ij}^-)$  is contained in  $\hat{\mathcal{L}}_{ij}^- := \hat{\mathcal{U}}_{ij}^{-1} \cup \hat{\mathcal{U}}_{ij}^{-2} \cup \hat{\mathcal{U}}_{ij}^{-3} \cup \hat{\mathcal{U}}_{ij}^{-4} \cup \hat{\mathcal{U}}_{ij}^{-5}$  where

$$\begin{aligned} \hat{\mathcal{U}}_{ij}^{-2} & = \{(\pi_i, \underline{\pi}_j, \underline{f}_{ij}, l_{ij}, 1) \in \mathbb{R}^5 : (\pi_i, -l_{ij}) \in \hat{\mathcal{V}}(-H_{ij}\underline{f}_{ij}, \underline{\pi}_j, \max\{\underline{\pi}_i, \underline{\pi}_j r_{ij}\}, \min\{\bar{\pi}_i, \underline{\pi}_j \bar{r}_{ij}\})\} \\ \hat{\mathcal{U}}_{ij}^{-3} & = \{(\pi_i, \bar{\pi}_j, \underline{f}_{ij}, l_{ij}, 1) \in \mathbb{R}^5 : (\pi_i, -l_{ij}) \in \hat{\mathcal{V}}(-H_{ij}\underline{f}_{ij}, \bar{\pi}_j, \max\{\underline{\pi}_i, \bar{\pi}_j r_{ij}\}, \min\{\bar{\pi}_i, \bar{\pi}_j \bar{r}_{ij}\})\} \end{aligned}$$

$$\begin{aligned}\hat{\mathcal{U}}_{ij}^{-4} &= \{(\pi_i, \pi_j, \underline{f}_{ij}, l_{ij}, 1) \in \mathbb{R}^5 : (\pi_j, -l_{ij}) \in \hat{\mathcal{W}}(-H_{ij}\underline{f}_{ij}, \underline{\pi}_i, \max\{\underline{\pi}_j, \underline{\pi}_i/\bar{r}_{ij}\}, \min\{\bar{\pi}_j, \bar{\pi}_i/r_{ij}\})\} \\ \hat{\mathcal{U}}_{ij}^{-5} &= \{(\bar{\pi}_i, \pi_j, \underline{f}_{ij}, l_{ij}, 1) \in \mathbb{R}^5 : (\pi_j, -l_{ij}) \in \hat{\mathcal{W}}(-H_{ij}\underline{f}_{ij}, \bar{\pi}_i, \max\{\underline{\pi}_j, \bar{\pi}_i/\bar{r}_{ij}\}, \min\{\bar{\pi}_j, \bar{\pi}_i/r_{ij}\})\}.\end{aligned}$$

Moreover,  $\text{conv}(\hat{\mathcal{L}}_{ij}^-)$  is SOCr.

Now, it is relatively easy to give a formal description of the outer-approximation of  $\text{conv}(\hat{\mathcal{L}}_{ij})$ . In Appendix B, we provide an extended formulation for this SOCr set.

## 4 Solution Methodology

In Section 3, we presented our main results on the nonconvex feasible sets for pipes and compressors. In this section, we will describe how we can solve the multi-period gas transportation and storage problem (6) by using them. We summarize our two-step solution framework in Algorithm 1. The input of our algorithm is the choice of the mixed-integer convex relaxation for the nonconvex MINLP problem (6). The tolerance of the convex relaxation is denoted by  $\epsilon$ . We also denote the  $\epsilon$ -optimal values of the binary and continuous variables produced by this relaxation as  $x^*$  and  $y^*$ , respectively. In Step 1 of Algorithm 1, a mixed-integer convex relaxation of our choice is solved to optimality. The dual bound for this relaxation provides a lower bound on the objective value of problem (6). In order to obtain (locally) optimal solutions, all the optimal binary values  $x^*$  produced by the relaxation are fixed, which reduces the nonconvex MINLP problem (6) to a nonlinear program (NLP). By passing the optimal continuous values  $y^*$  produced by the relaxation as the initial point, we solve this program with a local interior point solver in Step 4. If the solver converges to a (locally) optimal solution, which is also feasible for problem (6), we obtain an upper bound on its optimal objective value. By using these lower and upper bounds, the relative optimality gap in percentages is then calculated.

---

### Algorithm 1 MINLP

---

**Require:** `convexRelaxation`.

**Ensure:** Primal and dual bounds for problem (6), the relative optimality gap in percentages.

- 1: Solve `convexRelaxation` of problem (6).
  - 2: Obtain  $\epsilon$ -optimal solutions  $x^*$  and  $y^*$  produced by `convexRelaxation`.
  - 3: Assign the dual bound of `convexRelaxation` to  $LB$ .
  - 4: Solve problem (6) by fixing  $x^*$  and passing  $y^*$  as an initial point.
  - 5: Assign the primal bound of problem (6) to  $UB$ .
  - 6: Assign the relative optimality  $(1 - LB/UB)\%$  to  $Gap$ .
  - 7: **return**  $LB, UB, Gap$ .
- 

We conclude this section by providing the mixed-integer convex relaxations that can be used within Algorithm 1 to solve the multi-period gas transportation and storage problem (6). These relaxations differ based on the choice of the convexification approaches for the nonconvex Weymouth set  $\mathcal{X}$ , which are explained in Section 3.2. Note that we use the mixed-integer SOCr set described as in Theorem 3 for the nonconvex feasible set for compressors. We consider the following cases for `convexRelaxation` in Algorithm 1 with respect to the convexification of the Weymouth set:

- R1: The MISOCP relaxation with the convex hull as described in Section 3.2.1.
- R2: The MISOCP relaxation with the SOCr outer-approximation proposed by [20] as described in Section 3.2.2.
- R3: The MILP relaxation with the polyhedral outer-approximation adapted from [12] as described in Section 3.2.2.

## 5 Numerical Experiments

In this section, we present our computational study conducted on various GasLib test instances from the literature [41, 42]. We focus on short-term gas network operations and let  $|\mathcal{T}| = 24$ . Note that demand parameters in GasLib instances are given for a single period. Thus, we generate a new demand dataset by using the 24-hour gas demand data in Schwele et al. [29] such that the single-period demand from GasLib instances is the average gas demand within the planning horizon. Table 1 shows the cardinality of gas network elements for all the test instances used in the computational study.

Instance	$ \mathcal{N} $	$ \mathcal{N}_{source} $	$ \mathcal{N}_{sink} $	$ \mathcal{P} $	$ \mathcal{C} $	$ \mathcal{V} $	$ \mathcal{R} $
Gaslib-11	11	3	3	8	2	0	1
Gaslib-24	24	3	5	21	3	1	0
Gaslib-39	39	2	5	28	2	4	7
Gaslib-40	40	3	29	39	6	0	0
Gaslib-134	134	3	45	131	1	1	0

**Table 1:** The network elements in GasLib instances.

## 5.1 Computational Setting

All computational experiments are conducted on a 64-bit workstation with two Intel(R) Xeon(R) Gold 6248R CPU (3.00GHz) processors. The workstation runs on the Windows operations system and has 256 GB 2993 Mhz RAM. All mixed-integer convex relaxations for the multi-period gas storage optimization problem are solved by using the Gurobi Optimizer 11.0.1 [43]. The `BarHomogeneous` and `BarConvTol` parameters are set to 1 and  $5 \times 10^{-6}$  in Gurobi, respectively. After fixing the binary variables obtained from these relaxations, the resulting NLP is solved by the interior point solver Ipopt 3.11.1 [44]. For these NLPs, the `bound_relax_factor` and `max_iter` parameters are set to 0 and  $5 \times 10^4$  in Ipopt, respectively. We also compare the computational performance of our approaches by solving the nonconvex MINLP problem (6) with the global optimization solver BARON [45]. The time limit within each solver is set to one hour. All computational experiments are measured in seconds.

In order to assess the scalability of our approaches, we also stress the gas network by scaling the gas demand from the set  $\{0.1, 0.5, 1.0, 1.5\}$  for each test instance. Moreover, we also conduct our experiments under different objectives that are used in the gas network optimization problems. In particular, we minimize the following objective functions with positive cost parameters:

- $g_1 = \sum_{(i,j) \in \mathcal{C}} \sum_{t \in \mathcal{T}} (C_{ij}^{fc} |l_{ijt}| + C_{ij}^{up} u_{ijt}) + \sum_{i \in \mathcal{N}} \sum_{j \in \mathcal{S}(i)} \sum_{t \in \mathcal{T}} C_j^{wd} s_{kt}^-$ .
- $g_2 = \sum_{(i,j) \in \mathcal{C}} \sum_{t \in \mathcal{T}} (\gamma_1 |\pi_{it} - \pi_{jt}| + \gamma_2 |(\pi_{it} - \pi_{i,t-1}) - (\pi_{jt} - \pi_{j,t-1})|)$ .
- $g_3 = \sum_{(i,j) \in \mathcal{C}} \sum_{t \in \mathcal{T}} C_{ij}^{fc} |l_{ijt}|$ .

We note that the absolute values in these objective functions can be easily handled by common linearization approaches. The objective function  $g_1$  and  $g_3$  are the operational costs whereas  $g_2$  is a simplified version of energy consumption by compressors, see, e.g., [31]. We present our computational results by presenting the following metrics that are obtained within Algorithm 1:

- Dual bound: Lower bound obtained by `convexRelaxation`.
- Primal bound: Upper bound obtained by the NLP.
- Relaxation time: Wall-clock time in `convexRelaxation`.
- Total time: Total wall-clock time.
- Gap (%): The relative optimality gap in percentages.

The abbreviation “inf” (under column “Dual bound”) is used if the mixed-integer convex relaxation is proven to be infeasible. Similarly, under “Primal bound” columns, we use the abbreviation “inf” if the local solver converges to a locally infeasible solution. Under “Relaxation time” column, we use the abbreviation “TL” if the one-hour time limit has been reached.

Next, we explain the implementation of the disjunctive formulations of (6) for Gurobi and BARON. For each  $(i, j) \in \mathcal{A}$ , we define two binary variables  $x_{ij}^+$  and  $x_{ij}^-$  that satisfy the relation  $x_{ij} = x_{ij}^+ + x_{ij}^-$  where  $x_{ij} \in [0, 1]$ . For both Gurobi and BARON, we replace the disjunctive formulations given by constraints (2a), (6g) and (6h) for each (control) valve  $(i, j) \in \mathcal{A} \setminus \mathcal{C}$  by the following system of linear equations:

$$\begin{aligned}
\pi_j - r_{ij}\pi_i &\geq (\underline{\pi}_j - r_{ij}\bar{\pi}_i)(1 - x_{ij}^+), \quad \pi_j - \bar{r}_{ij}\pi_i \leq (\bar{\pi}_j - \bar{r}_{ij}\underline{\pi}_i)(1 - x_{ij}^+) & (i, j) \in \mathcal{A} \setminus \mathcal{C} \\
\pi_i - r_{ij}\pi_j &\geq (\underline{\pi}_i - r_{ij}\bar{\pi}_j)(1 - x_{ij}^-), \quad \pi_i - \bar{r}_{ij}\pi_j \leq (\bar{\pi}_i - \bar{r}_{ij}\underline{\pi}_j)(1 - x_{ij}^-) & (i, j) \in \mathcal{A} \setminus \mathcal{C} \\
x_{ij}^- f_{ij} &\leq f_{ij} \leq \bar{f}_{ij} x_{ij}^+ & (i, j) \in \mathcal{A} \setminus \mathcal{C}.
\end{aligned}$$

For the global solver BARON, we also recast the nonconvex system given by constraints (2a), (3a), (6g)-(6j) for each compressor  $(i, j) \in \mathcal{C}$  by the following system of nonlinear equations:

$$l_{ij} = H_{ij}((\pi_i/\pi_j)^{\hat{\kappa}} x_{ij}^+ + (\pi_j/\pi_i)^{\hat{\kappa}} x_{ij}^- - 1) f_{ij} \quad (i, j) \in \mathcal{C} \quad (8a)$$

$$\pi_j - r_{ij}\pi_i \geq (\underline{\pi}_j - r_{ij}\bar{\pi}_i)(1 - x_{ij}^+), \quad \pi_j - \bar{r}_{ij}\pi_i \leq (\bar{\pi}_j - \bar{r}_{ij}\underline{\pi}_i)(1 - x_{ij}^+) \quad (i, j) \in \mathcal{C} \quad (8b)$$

$$\pi_i - r_{ij}\pi_j \geq (\underline{\pi}_i - r_{ij}\bar{\pi}_j)(1 - x_{ij}^-), \quad \pi_i - \bar{r}_{ij}\pi_j \leq (\bar{\pi}_i - \bar{r}_{ij}\underline{\pi}_j)(1 - x_{ij}^-) \quad (i, j) \in \mathcal{C} \quad (8c)$$

$$x_{ij}^- f_{ij} \leq f_{ij} \leq \bar{f}_{ij} x_{ij}^+ \quad (i, j) \in \mathcal{C}. \quad (8d)$$

In Table 2, we summarize the different formulations that are used in our computational experiments. We remind the reader that we use the MISOCP relaxation of each formulation for R1, R2 and R3 in Gurobi.

Nonconvex sets	R1	R2	R3	BARON
Weymouth set ( $\mathcal{X}_{ij}$ ) for pipes	Conv( $\mathcal{X}_{ij}$ ) (Theorem 1)	$\mathcal{X}_{\text{socr}}$	$\mathcal{X}_{\text{poly}}$	$\mathcal{X}_{ij}$
Compression set ( $\mathcal{L}_{ij}$ ) for compressors	$\mathcal{Y}_{ij}$ (Theorem 3)			(8)

**Table 2:** The summary of different formulations used in solvers.

## 5.2 Computational Results

In this section, we present the results of our computational study. In particular, we consider small-scale gas networks with 11, 24, 39, and 40 nodes and medium-scale real-world gas networks with 134. For test networks, a single nomination is provided. In Tables 3, 4, 5 and 6, we report our detailed results for small-scale networks. For GasLib-134, there are multiple nominations provided in three categories, namely, warm, mild and cold. We pick a single nomination from each category and present our computational results under different temperature conditions for GasLib-134. In particular, we pick nominations “2015-08-23”, “2015-05-24” and “2016-02-10” for mild, warm and cold temperatures, respectively. In Tables 7, 8, and 9 and 6, we report our detailed results for GasLib-134 under warm, mild and cold nominations, respectively.

For the GasLib-11 network, we observe that the performance of R1 is consistently better than other methods in terms of optimality gaps for all instances. We also observe that BARON reaches to the time limit and is unable to provide near-global solutions under the objectives  $g_1$  and  $g_3$  although the primal bounds of BARON are very close to the dual bounds produced by the convex relaxations. Although BARON provides better primal bounds under  $g_2$  compared to the relaxation methods, its computational performance decreases and cannot prove optimality under the time limit as the congestion level increases. We see that although the differences in total time are mostly negligible among all convex relaxation methods, R2 and R3 are computationally faster than R1. However, our method consistently outperforms these methods in terms of both dual and primal bounds and is able to provide near-global solutions for all instances.

For the GasLib-24 network, we restrict ourselves to the positive gas flows for pipes and exclude R2 (see, Remark 1 for unidirectional flows). We see that convex relaxation methods outperform BARON and are able to produce near-global solutions under the objectives  $g_1$  and  $g_3$ . Moreover, our method R1 is computationally faster than R3 for all instances whereas BARON reaches the time limit. Under the objective  $g_2$ , we observe that BARON is able to terminate within the time limit and produce near-global solutions. On the other hand, convex relaxation methods are also able to produce the same solutions as BARON; however, they cannot prove global optimality due to the locally optimal solutions they produce. Still, the optimality gaps produced by these relaxations decrease considerably as the stress level in the network increases.

For the GasLib-39 network, we first note that we encounter some persistent issues with BARON. In particular, BARON gives inconsistent results for all instances. For example, BARON claims that the instances under stress levels 0.1 and 0.5 are infeasible under the objective  $g_3$  whereas it is able to produce primal bounds under  $g_1$  and  $g_2$  for the same instances. The same infeasibility issue also occurs as the network congestion increases under the objectives  $g_1$  and  $g_2$ . In terms of dual bounds, the convex relaxation methods produce similar results. In terms of primal bounds, R1 consistently produces high-quality feasible solutions and better optimality gaps compared to other relaxation methods. In the local solver, we also observe that there are cases where both R2 and R3 converge to a point of local infeasibility when initiated with the starting solutions produced by these relaxations. Still, R1 offers high-quality warm starting points for local solvers for all instances.

For the GasLib-40 network, we encounter the same issues with BARON. Interestingly, it claims false infeasibility for all feasible instances. We try to overcome this by solving the underlying problem in a shorter planning horizon and decreasing the stress levels. Still, BARON falsely states upon termination that these instances are infeasible. Still, it is able to claim infeasibility within the time limit under the stress level of 1.5. For most of the instances, R1 is able to produce considerably better optimality gaps compared to other methods within the time limit. Moreover, it also produces considerably tighter dual bounds compared to other relaxation methods under the objective  $g_2$  for low congested networks. All convex relaxations detect infeasibility within the time limit; however, R1 and R3 are computationally faster than R2.

Stress	Solver	$g_1$					$g_2$					$g_3$				
		Dual bound	Primal bound	Relaxation time	Total time	Gap (%)	Dual bound	Primal bound	Relaxation time	Total time	Gap (%)	Dual bound	Primal bound	Relaxation time	Total time	Gap (%)
0.1	R1	<b>11585.95</b>	11585.95	7.34	21.13	<b>0.00</b>	23.91	24.39	4.39	5.50	1.98	<b>332.10</b>	332.10	2.27	2.88	<b>0.00</b>
	R2	11585.91	11663.14	5.89	7.78	0.66	23.19	24.39	3.23	4.22	4.92	332.07	334.09	1.41	2.74	0.87
	R3	11585.91	11586.45	1.70	3.67	0.00	23.19	inf	1.16	5.17	-	332.07	inf	1.22	3.22	-
	BARON	11393.64	11585.95	-	TL	1.66	<b>24.39</b>	24.39	-	33.77	<b>0.01</b>	134.84	332.10	-	TL	59.40
0.5	R1	<b>12985.73</b>	12986.74	7.22	8.91	<b>0.01</b>	27.68	29.09	3.96	5.30	4.86	<b>1660.49</b>	1660.49	1.94	3.39	<b>0.00</b>
	R2	<b>12985.73</b>	12988.73	1.51	2.72	0.02	27.68	29.12	2.75	3.98	4.94	1660.11	1660.49	1.09	2.51	0.02
	R3	<b>12985.73</b>	12987.19	1.13	2.87	0.01	27.68	30.35	2.03	4.13	8.82	<b>1660.49</b>	1660.49	1.09	2.17	<b>0.00</b>
	BARON	12009.43	12985.73	-	TL	7.52	<b>28.34</b>	28.61	-	TL	<b>0.94</b>	665.27	1660.49	-	TL	59.94
1.0	R1	<b>14735.46</b>	14735.46	4.30	6.39	<b>0.00</b>	<b>33.81</b>	35.83	65.99	67.97	<b>5.62</b>	<b>3320.98</b>	3320.98	1.99	4.72	<b>0.00</b>
	R2	<b>14735.46</b>	14740.06	1.43	3.30	0.03	33.32	35.66	58.55	62.75	6.57	<b>3320.98</b>	3320.98	1.42	2.73	<b>0.00</b>
	R3	<b>14735.46</b>	14735.84	1.10	2.42	0.00	32.42	35.52	20.45	21.67	8.74	<b>3320.98</b>	inf	1.04	2.13	-
	BARON	12743.96	14738.38	-	TL	13.53	33.11	35.67	-	TL	7.16	1324.65	3320.98	-	TL	60.11
1.5	R1	16485.19	16493.52	4.18	7.12	0.05	<b>45.65</b>	46.39	73.85	75.18	<b>1.58</b>	<b>4981.47</b>	4981.47	1.73	3.05	<b>0.00</b>
	R2	<b>16485.26</b>	16508.25	1.19	3.16	0.14	<b>45.65</b>	46.39	47.70	50.12	<b>1.58</b>	<b>4981.47</b>	4981.47	1.31	2.41	<b>0.00</b>
	R3	16485.19	16492.95	1.37	4.22	<b>0.05</b>	43.36	46.39	16.04	17.25	6.52	<b>4981.47</b>	4981.47	1.37	2.91	<b>0.00</b>
	BARON	13816.16	16485.18	-	TL	16.19	44.30	45.70	-	TL	3.06	2273.25	4981.47	-	TL	54.37

**Table 3: Computational results on GasLib-11**

Stress	Solver	$\beta_1$					$\beta_2$					$\beta_3$				
		Dual bound	Primal bound	Relaxation time	Total time	Gap (%)	Dual bound	Primal bound	Relaxation time	Total time	Gap (%)	Dual bound	Primal bound	Relaxation time	Total time	Gap (%)
0.1	R1	<b>17934.98</b>	17934.98	1.97	5.71	<b>0.00</b>	<b>31.28</b>	35.04	2.04	3.36	10.74	<b>1048.60</b>	1048.60	1.97	15.30	<b>0.00</b>
	R3	<b>17934.98</b>	17934.98	2.03	11.08	<b>0.00</b>	<b>31.28</b>	35.04	2.02	3.37	10.74	<b>1048.60</b>	1048.60	2.00	15.48	<b>0.00</b>
	BARON	17040.26	17934.98	-	TL	4.99	<b>31.28</b>	31.28	-	2.45	<b>0.00</b>	119.68	1048.60	-	TL	88.59
0.5	R1	<b>22258.90</b>	22258.90	1.98	5.84	<b>0.00</b>	<b>30.04</b>	32.13	2.24	5.63	6.51	<b>5242.98</b>	5242.98	1.99	5.80	<b>0.00</b>
	R3	<b>22258.90</b>	22258.90	1.95	7.08	<b>0.00</b>	<b>30.04</b>	32.13	2.26	6.38	6.51	<b>5242.98</b>	5242.98	1.92	5.62	<b>0.00</b>
	BARON	17380.53	22258.90	-	TL	21.92	<b>30.04</b>	30.04	-	17.94	<b>0.01</b>	389.67	5242.98	-	TL	92.57
1.0	R1	<b>27663.79</b>	27663.79	2.02	5.94	<b>0.00</b>	<b>31.60</b>	31.85	2.02	5.86	0.78	<b>10485.97</b>	10485.97	1.95	6.73	<b>0.00</b>
	R3	<b>27663.79</b>	27663.79	2.05	5.97	<b>0.00</b>	<b>31.60</b>	31.85	2.27	5.45	0.78	<b>10485.97</b>	10485.97	1.92	6.77	<b>0.00</b>
	BARON	17729.56	27663.79	-	TL	35.91	31.59	31.60	-	11.98	<b>0.01</b>	526.13	10485.97	-	TL	94.98
1.5	R1	<b>33068.69</b>	33068.69	1.99	4.72	<b>0.00</b>	<b>35.61</b>	35.96	2.29	9.23	0.98	<b>15728.95</b>	15728.95	1.92	5.29	<b>0.00</b>
	R3	<b>33068.69</b>	33068.69	1.95	5.80	<b>0.00</b>	<b>35.61</b>	35.96	2.57	6.08	0.98	<b>15728.95</b>	15728.95	1.94	5.45	<b>0.00</b>
	BARON	18133.35	33068.69	-	TL	45.16	35.60	35.61	-	15.99	<b>0.01</b>	792.86	15728.95	-	TL	94.96

Table 4: Computational results on GasLib-24

Stress	Solver	$g_1$					$g_2$					$g_3$				
		Dual bound	Primal bound	Relaxation time	Total time	Gap (%)	Dual bound	Primal bound	Relaxation time	Total time	Gap (%)	Dual bound	Primal bound	Relaxation time	Total time	Gap (%)
0.1	R1	<b>13018.55</b>	13018.55	5.02	13.54	<b>0.00</b>	<b>13.09</b>	15.99	20.63	37.92	18.12	<b>1673.82</b>	1673.82	4.43	14.79	<b>0.00</b>
	R2	<b>13018.55</b>	13031.37	2.33	11.80	0.10	<b>13.09</b>	32.27	4.58	360.75	59.44	<b>1673.82</b>	1673.82	2.22	30.17	<b>0.00</b>
	R3	<b>13018.55</b>	inf	1.72	13.49	-	<b>13.09</b>	inf	1.89	19.26	-	1673.81	1673.82	1.71	17.90	<b>0.00</b>
	BARON	11344.73	13018.55	-	TL	12.86	<b>13.09</b>	13.12	-	TL	<b>0.26</b>	-	inf	-	81.95	-
0.5	R1	<b>20148.75</b>	20148.75	4.50	10.74	<b>0.00</b>	<b>13.09</b>	27.34	2619.95	2642.07	52.12	<b>8369.08</b>	8369.08	4.40	14.03	<b>0.00</b>
	R2	<b>20148.75</b>	inf	6.79	19.66	-	<b>13.09</b>	34.86	TL	3663.08	62.45	<b>8369.08</b>	8369.08	2.54	38.86	<b>0.00</b>
	R3	<b>20148.75</b>	20268.14	1.71	38.30	0.59	<b>13.09</b>	28.78	2.09	1133.24	54.52	<b>8369.08</b>	8369.08	1.74	20.60	<b>0.00</b>
	BARON	11779.67	20148.75	-	TL	41.54	<b>13.09</b>	14.68	-	TL	<b>10.81</b>	-	inf	-	42.66	-
1.0	R1	<b>29061.50</b>	29080.17	5.53	26.19	<b>0.06</b>	15.03	16.29	TL	3662.87	<b>7.70</b>	<b>16738.15</b>	16738.15	5.08	16.00	<b>0.00</b>
	R2	<b>29061.50</b>	29138.14	5.63	37.73	0.26	14.98	29.90	TL	3645.26	49.90	<b>16738.15</b>	inf	2.76	14.31	-
	R3	<b>29061.50</b>	inf	1.81	12.27	-	13.80	34.95	2.75	292.89	60.52	<b>16738.15</b>	inf	1.80	10.05	-
	BARON	12323.35	29069.24	-	TL	57.61	<b>16.13</b>	18.93	-	TL	14.80	0.00	16738.15	-	TL	100.00
1.5	R1	<b>37974.25</b>	37985.86	TL	3630.18	<b>0.03</b>	<b>20.16</b>	23.91	TL	3786.89	<b>15.68</b>	<b>25107.23</b>	25107.23	114.36	139.28	<b>0.00</b>
	R2	<b>37974.25</b>	inf	177.45	189.00	-	19.48	32.70	TL	3729.74	40.43	<b>25106.97</b>	inf	2.43	25.62	-
	R3	<b>37974.25</b>	38607.72	1.59	17.36	1.64	18.81	32.30	324.08	353.57	41.78	<b>25107.23</b>	25107.23	1.58	23.36	<b>0.00</b>
	BARON	inf	inf	-	174.49	-	-	inf	-	13.90	-	724.00	25107.22	-	TL	97.12

Table 5: Computational results on GasLib-39

Stress	Solver	g1					g2					g3				
		Dual bound	Primal bound	Relaxation time	Total time	Gap (%)	Dual bound	Primal bound	Relaxation time	Total time	Gap (%)	Dual bound	Primal bound	Relaxation time	Total time	Gap (%)
0.1	R1	30402.54	30402.76	TL	3652.87	0.00	<b>0.57</b>	10.55	TL	3626.27	<b>94.63</b>	2183.14	2197.27	970.01	1006.11	<b>0.64</b>
	R2	30402.49	30557.82	1224.97	1272.33	0.51	0.51	66.50	TL	3633.55	99.24	2178.19	2945.06	TL	3690.41	26.04
	R3	<b>30402.62</b>	30402.76	2.95	49.94	<b>0.00</b>	0.05	3.98	4.31	59.93	98.65	<b>2183.22</b>	3164.83	3.22	60.60	31.02
	BARON	-	inf	-	533.76	-	-	inf	-	381.03	-	-	inf	-	104.43	-
0.5	R1	<b>39653.82</b>	39653.82	8.17	19.97	<b>0.00</b>	<b>19.30</b>	188.20	TL	3648.39	89.74	<b>10916.85</b>	10916.85	630.30	684.10	<b>0.00</b>
	R2	<b>39653.82</b>	39653.82	101.83	255.37	<b>0.00</b>	12.46	69.18	TL	3681.64	<b>81.98</b>	10862.79	12343.13	TL	3706.31	11.99
	R3	39651.30	39653.82	3.18	9.17	0.01	1.37	67.79	3.07	91.59	97.97	10914.33	10916.85	3.03	9.06	0.02
	BARON	-	inf	-	69.95	-	-	inf	-	82.79	-	-	inf	-	202.82	-
1.0	R1	51217.52	51217.64	107.06	114.30	0.00	-	-	TL	3656.69	-	<b>21833.70</b>	22997.54	TL	4277.62	5.06
	R2	<b>51217.62</b>	51217.64	TL	3631.30	<b>0.00</b>	-	-	TL	3618.00	-	21833.61	23425.75	1873.25	1964.20	6.80
	R3	51217.55	51217.64	3.04	11.64	0.00	<b>59.31</b>	271.03	4.16	44.50	<b>78.12</b>	21833.61	22296.61	3.26	65.98	<b>2.08</b>
	BARON	-	inf	-	127.04	-	-	inf	-	100.29	-	-	inf	-	86.15	-
1.5	R1	inf	-	9.23	9.23	-	inf	-	13.32	13.32	-	inf	-	10.56	-	-
	R2	-	-	TL	3612.88	-	inf	-	161.81	161.81	-	inf	-	258.62	258.62	-
	R3	inf	-	2.92	2.92	-	inf	-	2.84	2.84	-	inf	-	2.74	2.74	-
	BARON	-	inf	-	37.15	-	-	inf	-	230.32	-	-	inf	-	59.18	-

Table 6: Computational results on GasLib-40

Stress	Solver	$g_1$					$g_3$				
		Dual bound	Primal bound	Relaxation time	Total time	Gap (%)	Dual bound	Primal bound	Relaxation time	Total time	Gap (%)
0.1	R1	<b>5788.02</b>	5788.02	22.49	103.82	<b>0.00</b>	<b>158.35</b>	158.35	12.21	61.41	<b>0.00</b>
	R2	<b>5788.02</b>	5788.02	80.14	440.38	<b>0.00</b>	<b>158.35</b>	158.35	4.22	50.31	<b>0.00</b>
	R3	<b>5788.02</b>	5788.31	2.91	29.48	0.01	<b>158.35</b>	inf	2.81	158.39	-
	BARON	5706.12	5788.02	-	TL	1.41	37.77	158.35	-	TL	76.15
0.5	R1	<b>6468.08</b>	6468.08	33.04	108.32	<b>0.00</b>	<b>791.74</b>	791.74	11.08	57.16	<b>0.00</b>
	R2	<b>6468.08</b>	6468.08	83.02	326.09	<b>0.00</b>	<b>791.74</b>	791.74	4.83	35.11	<b>0.00</b>
	R3	<b>6468.08</b>	6468.08	3.13	302.65	<b>0.00</b>	<b>791.74</b>	inf	2.80	30.95	-
	BARON	5959.13	6468.08	-	TL	7.87	213.41	791.74	-	TL	73.05
1.0	R1	<b>7318.16</b>	7318.17	13.27	22.91	<b>0.00</b>	<b>1583.49</b>	1583.49	4.43	76.89	<b>0.00</b>
	R2	<b>7318.16</b>	7318.17	4.25	63.86	<b>0.00</b>	<b>1583.49</b>	inf	2.69	66.61	-
	R3	<b>7318.16</b>	7318.17	2.80	42.07	<b>0.00</b>	<b>1583.49</b>	1583.49	13.01	47.25	<b>0.00</b>
	BARON	6282.99	7318.17	-	TL	14.15	468.40	1583.49	-	TL	70.42
1.5	R1	<b>8168.25</b>	8168.25	14.61	57.90	<b>0.00</b>	<b>2375.23</b>	2375.23	15.38	132.75	<b>0.00</b>
	R2	<b>8168.25</b>	8168.25	5.20	50.44	<b>0.00</b>	<b>2375.23</b>	2375.23	5.11	75.13	<b>0.00</b>
	R3	<b>8168.25</b>	8168.25	2.96	49.44	<b>0.00</b>	<b>2375.23</b>	inf	2.81	39.43	-
	BARON	6620.45	8168.25	-	TL	18.95	742.09	2375.23	-	TL	68.76

**Table 7:** Computational results on GasLib-134 under warm nomination

Stress	Solver	g1					g3				
		Dual bound	Primal bound	Relaxation time	Total time	Gap (%)	Dual bound	Primal bound	Relaxation time	Total time	Gap (%)
0.1	R1	<b>5768.87</b>	5768.87	90.78	222.79	<b>0.00</b>	<b>140.89</b>	140.89	12.40	37.25	<b>0.00</b>
	R2	<b>5768.87</b>	inf	88.90	197.99	-	<b>140.89</b>	140.91	4.67	59.23	0.01
	R3	<b>5768.87</b>	5768.87	2.90	60.08	<b>0.00</b>	<b>140.89</b>	inf	2.68	95.96	-
	BARON	5694.70	5768.87	-	TL	1.29	48.18	140.89	-	TL	65.80
0.5	R1	<b>6372.35</b>	6372.35	47.97	59.59	<b>0.00</b>	<b>704.47</b>	704.47	11.40	88.23	<b>0.00</b>
	R2	<b>6372.35</b>	6372.35	1360.48	1524.30	<b>0.00</b>	<b>704.47</b>	706.76	4.15	50.06	0.32
	R3	<b>6372.35</b>	6372.35	3.24	204.03	<b>0.00</b>	<b>704.47</b>	inf	2.78	25.18	-
	BARON	5909.59	6372.35	-	TL	7.26	190.81	704.47	-	TL	72.91
1.0	R1	<b>7126.70</b>	7126.71	12.23	60.37	<b>0.00</b>	<b>1408.94</b>	1408.94	13.56	74.83	<b>0.00</b>
	R2	<b>7126.70</b>	7126.71	5.01	16.16	<b>0.00</b>	<b>1408.94</b>	1408.95	4.40	44.09	0.00
	R3	<b>7126.70</b>	7128.98	2.69	87.34	0.03	<b>1408.94</b>	inf	2.80	17.25	-
	BARON	6200.02	7126.71	-	TL	13.00	382.52	1408.94	-	TL	72.85
1.5	R1	<b>7881.06</b>	7881.06	13.09	28.21	<b>0.00</b>	<b>2113.41</b>	2113.41	14.88	92.64	<b>0.00</b>
	R2	<b>7881.06</b>	7881.06	5.04	32.70	<b>0.00</b>	<b>2113.41</b>	2113.41	4.96	45.44	<b>0.00</b>
	R3	<b>7881.06</b>	7881.06	2.78	27.38	<b>0.00</b>	<b>2113.41</b>	inf	2.93	37.68	-
	BARON	6491.19	7881.06	-	TL	17.64	521.14	2113.41	-	TL	75.34

**Table 8:** Computational results on GasLib-134 under mild nomination

Stress	Solver	$g_1$					$g_3$				
		Dual bound	Primal bound	Relaxation time	Total time	Gap (%)	Dual bound	Primal bound	Relaxation time	Total time	Gap (%)
0.1	R1	<b>5871.64</b>	5871.64	127.08	207.25	<b>0.00</b>	<b>223.62</b>	223.62	12.32	73.45	<b>0.00</b>
	R2	<b>5871.64</b>	inf	36.27	236.52	-	<b>223.62</b>	inf	4.26	49.70	-
	R3	<b>5871.64</b>	5871.64	2.97	23.85	<b>0.00</b>	<b>223.62</b>	inf	2.69	402.43	-
	BARON	-	inf	-	13.67	-	143.99	223.62	-	TL	35.61
0.5	R1	6886.19	6886.20	12.32	102.78	0.00	<b>1118.09</b>	1118.09	12.73	128.06	<b>0.00</b>
	R2	<b>6886.20</b>	6886.20	67.93	149.98	<b>0.00</b>	<b>1118.09</b>	inf	4.17	299.52	-
	R3	<b>6886.20</b>	6886.20	3.03	30.02	<b>0.00</b>	<b>1118.09</b>	inf	2.80	124.10	-
	BARON	-	inf	-	157.98	-	766.03	1118.09	-	TL	31.49
1.0	R1	<b>8154.39</b>	8154.39	13.44	106.25	<b>0.00</b>	<b>2236.18</b>	2236.18	12.62	134.56	<b>0.00</b>
	R2	8154.38	8154.39	5.34	33.20	0.00	<b>2236.18</b>	inf	4.82	234.28	-
	R3	8154.38	8154.39	2.85	31.31	0.00	<b>2236.18</b>	inf	2.75	37.82	-
	BARON	-	inf	-	55.34	-	1356.40	2236.18	-	TL	39.34
1.5	R1	<b>9422.59</b>	9422.59	190.59	223.44	<b>0.00</b>	<b>3354.27</b>	3354.27	13.92	74.51	<b>0.00</b>
	R2	<b>9422.59</b>	11413.30	60.23	91.12	17.44	<b>3354.27</b>	inf	5.66	194.27	-
	R3	9422.58	9422.59	2.97	61.81	0.00	<b>3354.27</b>	inf	2.85	117.10	-
	BARON	-	inf	-	77.63	-	1512.13	12014.83	-	TL	87.41

**Table 9:** Computational results on GasLib-134 under cold nomination)

For the GasLib-134 network, we present our results under different nominations. We note that we encounter inconsistency issues with BARON. Interestingly, it produces inconsistent primal and dual bounds under the objective  $g_2$ . Thus, we omit them from our computational results. Although BARON reaches the time limit under warm and mild nominations, it is able to produce consistent results. However, it falsely claims infeasibility under the objective  $g_1$  in Table 9 although it is able to give consistent primal bounds under the objective  $g_3$  for cold nomination. All convex relaxation methods terminate within the time limit. Among these methods, R1 consistently produces near-global solutions for all instances under each nomination. Also, we observe that there are cases where both R2 and R3 converge to a point of infeasibility in the local solver whereas R1 provides high-quality warm starting points for all instances.

We summarize our computational results as follows: BARON is able to provide consistently dual and primal bounds for GasLib-11 and GasLib-24; however, we encounter some persistent inconsistency and infeasibility issues with BARON as the gas network gets more complex. Under the objective functions  $g_1$  and  $g_3$ , we see that the performance of the convex relaxations in terms of the optimality gap and total time is better than BARON for all instances. In particular, BARON returns considerably larger gaps as the stress level of the network increases. Moreover, R1 consistently provides tighter dual bounds for all instances and it also offers high-quality warm starting points for the local solver Ipopt compared to R2 and R3. We also observe that there are cases where both R2 and R3 converge to a point of local infeasibility when initiated with the starting solutions produced by these relaxations. We conclude that our relaxation method consistently leads to numerically more stable results in comparison with those methods from the literature and the global solver.

## 6 Conclusion

In conclusion, we studied the gas transportation and storage optimization problem, in which we explicitly considered the highly nonlinear and nonconvex inherent aspects due to gas physics as well as the discrete aspects due to the control decisions of active network elements. We studied the nonconvex sets induced by gas physics in detail and proposed MISOCP relaxations for this problem. In particular, our relaxation approach is based on the convex hull representations of the nonconvex sets as follows: We derived the exact convex hull formulation for the feasible (nonconvex) set for pipes and show that it is SOCr. We also provided the convex hull of the extreme points of the feasible (nonconvex) set for compressors and show that it is POWr. To fully utilize the state-of-the-art solver, we also proposed a second-order cone outer-approximation for this POWr set. Based on these relaxations, we also proposed an algorithmic framework to solve the problem. We tested our framework on multiple GasLib instances under different settings. Our computational results show that our method significantly outperforms the state-of-the-art global solver and other relaxation methods from the literature. Our approach consistently provides tight dual bounds and produces (near) global solutions as well as high-quality warm-starting points for local solvers ensuring numerical consistency and scalability.

There are several promising directions for future research. Extending our approach to integrated energy systems and incorporating uncertainty in demand and supply conditions could be an important area of study. Additionally, decomposition approaches for multi-period gas network optimization problems could improve computational efficiency and scalability.

**Acknowledgments.** This work was supported by the Scientific and Technological Research Council of Turkey under grant number 119M855.

## Appendix A Extreme Points of the Weymouth Set

For simplicity of notation, consider the set  $\mathcal{X}^+ = \{(x, y, z) \in \mathcal{B}^+ : x - y = wz^2\}$ , where  $\mathcal{B}^+ = \{(x, y, z) \in [x, \bar{x}] \times [y, \bar{y}] \times [0, \alpha] : 0 \leq x - y \leq \beta\}$  is a polytope such that  $\alpha \geq 0$  and  $\beta \geq 0$ . We have already established in Proposition 1 that  $\text{conv}(\mathcal{X}^+) = \{(x, y, z) \in \check{\mathcal{B}}^+ : x - y \geq wz^2\}$  for some polytope  $\check{\mathcal{B}}^+$ . In order to construct  $\check{\mathcal{B}}^+$ , we follow [38]: We first find the extreme points of the intersection of each edge of the polytope  $\mathcal{B}^+$  with the reverse convex constraint  $x - y \leq wz^2$  (Algorithm 2 provides the set of these points denoted as  $\mathcal{Q}^+$ ). Then, we obtain  $\check{\mathcal{B}}^+ = \text{conv}(\mathcal{Q}^+)$ .

Algorithm 2 can also be used to find the convex hull of the set  $\mathcal{X}^- = \{(x, y, z) \in \mathcal{B}^- : y - x = wz^2\}$ , where  $\mathcal{B}^- = \{(x, y, z) \in [x, \bar{x}] \times [y, \bar{y}] \times [\alpha', 0] : \beta' \leq x - y \leq 0\}$  such that  $\alpha' \leq 0$  and  $\beta' \leq 0$ . For this purpose, we first run Algorithm 2 with the input  $y, \bar{y}, x, \bar{x}, -\alpha', -\beta'$  to obtain  $\mathcal{Q}^+$ . Then, for any element  $(y, x, z) \in \mathcal{Q}^+$ , we have  $(x, y, -z) \in \mathcal{Q}^-$  such that  $\check{\mathcal{B}}^- = \text{conv}(\mathcal{Q}^-)$ .

---

**Algorithm 2** Extreme points of  $\check{\mathcal{B}}^+$ .

---

**Require:**  $x, \bar{x}, y, \bar{y}, \alpha, \beta$  such that  $0 < x \leq \bar{x}$ ,  $0 < y \leq \bar{y}$ ,  $\alpha \geq 0$ ,  $\beta \geq 0$ .

**Ensure:**  $\mathcal{Q}^+$

```
1:  $\mathcal{Q}^+ = \emptyset$ 
2: for  $(\tilde{x}, \tilde{y}) \in \text{extr}(\{(x, y) \in [x, \bar{x}] \times [y, \bar{y}] : 0 \leq x - y \leq \beta\})$  do
3:   Compute  $z' = \sqrt{(\tilde{x} - \tilde{y})/w}$ 
4:   if  $\alpha \leq z'$  then
5:      $\mathcal{Q}^+ = \mathcal{Q}^+ \cup \{(\tilde{x}, \tilde{y}, z'), (\tilde{x}, \tilde{y}, \alpha)\}$ 
6:   for  $\tilde{z} \in \{0, \alpha\}$  do
7:     for  $\tilde{x} \in \{x, \bar{x}\}$  do
8:       Compute  $y_1 = \max\{\underline{y}, \tilde{x} - \beta, \tilde{x} - w\tilde{z}^2\}$  and  $y_2 = \min\{\bar{y}, \tilde{x}\}$ 
9:       if  $y_1 \leq y_2$  then
10:         $\mathcal{Q}^+ = \mathcal{Q}^+ \cup \{(\tilde{x}, y_1, \tilde{z}), (\tilde{x}, y_2, \tilde{z})\}$ 
11:     for  $\tilde{y} \in \{y, \bar{y}\}$  do
12:       Compute  $x_1 = \max\{x, \tilde{y}\}$  and  $y_2 = \min\{\bar{x}, \tilde{y} + \beta, \tilde{y} + w\tilde{z}^2\}$ 
13:       if  $x_1 \leq x_2$  then
14:         $\mathcal{Q}^+ = \mathcal{Q}^+ \cup \{(x_1, \tilde{y}, \tilde{z}), (x_2, \tilde{y}, \tilde{z})\}$ 
15:     for  $d \in \{0, \beta\}$  do
16:       if  $d \leq w\tilde{z}^2$  then
17:         for  $\tilde{x} \in \{x, \bar{x}\}$  do
18:            $y' = \tilde{x} - d$ 
19:           if  $y \leq y' \leq \bar{y}$  then
20:             $\mathcal{Q}^+ = \mathcal{Q}^+ \cup \{(\tilde{x}, y', \tilde{z})\}$ 
21:         for  $\tilde{y} \in \{y, \bar{y}\}$  do
22:            $x' = \tilde{y} + d$ 
23:           if  $x \leq x' \leq \bar{x}$  then
24:             $\mathcal{Q}^+ = \mathcal{Q}^+ \cup \{(x', \tilde{y}, \tilde{z})\}$ 
25:   return  $\mathcal{Q}^+$ 
```

---

## Appendix B Extended Formulation for the SOCr Outer-Approximation of $\text{conv}(\mathcal{L}_{ij})$

By using Proposition 9 and Proposition 10, we provide a formal presentation of our results. We let  $n = 0.114$  and  $a > 0$ . For notational brevity, let us also introduce the following convex set with  $0 < b \leq \underline{x} \leq \bar{x}$ :

$$\begin{aligned} \check{\mathcal{V}}(a, b, \underline{x}, \bar{x}) &= \{(x, y, \lambda) \in \mathbb{R}_+^3 : \exists(u, v_1, v_2) \in \mathbb{R}_+^3 : u^2 \leq \lambda v_1, v_1^2 \leq \lambda v_2, b v_2^2 \leq \lambda x \\ &\quad y = a(u - \lambda), \underline{x}\lambda \leq x \leq \bar{x}\lambda \\ &\quad y \geq a\left(\frac{(\bar{x}/b)^n - (\underline{x}/b)^n}{\bar{x} - \underline{x}}\right)(x - \underline{x}\lambda) + a((\underline{x}/b)^n - 1)\lambda\}. \end{aligned}$$

Similarly, we define the following convex set with  $0 \leq x \leq \bar{x} < b$ :

$$\begin{aligned} \check{\mathcal{W}}(a, b, \underline{x}, \bar{x}) &= \{(x, y, \lambda) \in \mathbb{R}_+^3 : \exists(u, v_1, v_2, v_3) \in \mathbb{R}_+^4 : uv_1 \geq \lambda^2, \lambda v_2 \geq v_1^2, \lambda v_3 \geq v_2^2, ux \geq b v_3^2 \\ &\quad y = a(u - \lambda), \underline{x}\lambda \leq x \leq \bar{x}\lambda \\ &\quad y \leq a\left(\frac{(b/\bar{x})^n - (b/\underline{x})^n}{\bar{x} - \underline{x}}\right)(x - \underline{x}\lambda) + a((b/\underline{x})^n - 1)\lambda\}. \end{aligned}$$

Here,  $\check{\mathcal{V}}(a, b, \underline{x}, \bar{x})$  and  $\check{\mathcal{W}}(a, b, \underline{x}, \bar{x})$  are defined by rotated second-order conic and linear inequalities.

**Theorem 3.** *The following set provides an extended formulation for the SOCr outer-approximation of  $\text{conv}(\mathcal{L}_{ij})$ :*

$$\mathcal{Y}_{ij} := \left\{ \begin{array}{l} (\pi_i, \pi_j, f_{ij}, l_{ij}, x_{ij}, x_{ij}^+, x_{ij}^-) \in \mathbb{R}^7 \\ (\pi_i^{-5}, \pi_j^{-5}, f_{ij}^{-5}, l_{ij}^{-5}, \lambda_{ij}^{-5}) \in \mathbb{R}^5 \\ \vdots \\ (\pi_i^{+5}, \pi_j^{+5}, f_{ij}^{+5}, l_{ij}^{+5}, \lambda_{ij}^{+5}) \in \mathbb{R}^5 \end{array} \right. : \left\{ \begin{array}{l} \sum_{k=1}^{11} \lambda_{ij}^k = 1, \lambda_{ij}^k \geq 0, k = 1, \dots, 11 \\ x_{ij}^+ = \sum_{k=+1}^{+5} \lambda_{ij}^k, x_{ij}^- = \sum_{k=-5}^{-1} \lambda_{ij}^k \\ \pi_i = \sum_{k=-5}^{+5} \pi_i^k, \pi_j = \sum_{k=-5}^{+5} \pi_j^k \\ f_{ij} = \sum_{k=-5}^{+5} f_{ij}^k, l_{ij} = \sum_{k=-5}^{+5} l_{ij}^k \\ \pi_i \leq \pi_i \leq \bar{\pi}_i, \pi_j \leq \pi_j \leq \bar{\pi}_j, \underline{f}_{ij} x_{ij}^- \leq f_{ij} \leq \bar{f}_{ij} x_{ij}^+ \\ x_{ij} = x_{ij}^+ + x_{ij}^-, x_{ij}^+ \in [0, 1], x_{ij}^- \in [0, 1] \\ \pi_i \lambda_{ij}^0 \leq \pi_i^0 \leq \bar{\pi}_i \lambda_{ij}^0, \pi_j \lambda_{ij}^0 \leq \pi_j^0 \leq \bar{\pi}_j \lambda_{ij}^0, f_{ij}^0 = l_{ij}^0 = 0 \\ \pi_i \lambda_{ij}^{+1} \leq \pi_i^{+1} \leq \bar{\pi}_i \lambda_{ij}^{+1}, \pi_j \lambda_{ij}^{+1} \leq \pi_j^{+1} \leq \bar{\pi}_j \lambda_{ij}^{+1}, \underline{r}_{ij} \pi_i^{+1} \leq \pi_j^{+1} \leq \bar{r}_{ij} \pi_i^{+1}, f_{ij}^{+1} = l_{ij}^{+1} = 0 \\ (\pi_j^{+2}, l_{ij}^{+2}, \lambda_{ij}^{+2}) \in \check{\mathcal{V}}(H_{ij} \bar{f}_{ij}, \bar{\pi}_i, \max\{\underline{\pi}_j, \bar{\pi}_i \underline{r}_{ij}\}, \min\{\bar{\pi}_j, \bar{\pi}_i \bar{r}_{ij}\}), \pi_i^{+2} = \underline{\pi}_i \lambda_{ij}^{+2}, f_{ij}^{+2} = \bar{f}_{ij} \lambda_{ij}^{+2} \\ (\pi_j^{+3}, l_{ij}^{+3}, \lambda_{ij}^{+3}) \in \check{\mathcal{V}}(H_{ij} \bar{f}_{ij}, \bar{\pi}_i, \max\{\underline{\pi}_j, \bar{\pi}_i \underline{r}_{ij}\}, \min\{\bar{\pi}_j, \bar{\pi}_i \bar{r}_{ij}\}), \pi_i^{+3} = \bar{\pi}_i \lambda_{ij}^{+3}, f_{ij}^{+3} = \bar{f}_{ij} \lambda_{ij}^{+3} \\ (\pi_i^{+4}, l_{ij}^{+4}, \lambda_{ij}^{+4}) \in \check{\mathcal{W}}(H_{ij} \bar{f}_{ij}, \bar{\pi}_j, \max\{\underline{\pi}_i, \bar{\pi}_j / \bar{r}_{ij}\}, \min\{\bar{\pi}_i, \bar{\pi}_j / \underline{r}_{ij}\}), \pi_j^{+4} = \underline{\pi}_j \lambda_{ij}^{+4}, f_{ij}^{+4} = \bar{f}_{ij} \lambda_{ij}^{+4} \\ (\pi_i^{+5}, l_{ij}^{+5}, \lambda_{ij}^{+5}) \in \check{\mathcal{W}}(H_{ij} \bar{f}_{ij}, \bar{\pi}_j, \max\{\underline{\pi}_i, \bar{\pi}_j / \bar{r}_{ij}\}, \min\{\bar{\pi}_i, \bar{\pi}_j / \underline{r}_{ij}\}), \pi_j^{+5} = \bar{\pi}_j \lambda_{ij}^{+5}, f_{ij}^{+5} = \bar{f}_{ij} \lambda_{ij}^{+5} \\ \pi_i \lambda_{ij}^{-1} \leq \pi_i^{-1} \leq \bar{\pi}_i \lambda_{ij}^{-1}, \pi_j \lambda_{ij}^{-1} \leq \pi_j^{-1} \leq \bar{\pi}_j \lambda_{ij}^{-1}, \underline{r}_{ij} \pi_j^{-1} \leq \pi_i^{-1} \leq \bar{r}_{ij} \pi_j^{-1}, f_{ij}^{-1} = l_{ij}^{-1} = 0 \\ (\pi_i^{-2}, -l_{ij}^{-2}, \lambda_{ij}^{-2}) \in \check{\mathcal{V}}(-H_{ij} \underline{f}_{ij}, \underline{\pi}_j, \max\{\underline{\pi}_i, \underline{\pi}_j \underline{r}_{ij}\}, \min\{\bar{\pi}_i, \underline{\pi}_j \bar{r}_{ij}\}), \pi_j^{-2} = \underline{\pi}_j \lambda_{ij}^{-2}, f_{ij}^{-2} = \underline{f}_{ij} \lambda_{ij}^{-2} \\ (\pi_i^{-3}, -l_{ij}^{-3}, \lambda_{ij}^{-3}) \in \check{\mathcal{V}}(-H_{ij} \underline{f}_{ij}, \underline{\pi}_j, \max\{\underline{\pi}_i, \underline{\pi}_j \underline{r}_{ij}\}, \min\{\bar{\pi}_i, \underline{\pi}_j \bar{r}_{ij}\}), \pi_j^{-3} = \bar{\pi}_j \lambda_{ij}^{-3}, f_{ij}^{-3} = \underline{f}_{ij} \lambda_{ij}^{-3} \\ (\pi_j^{-4}, -l_{ij}^{-4}, \lambda_{ij}^{-4}) \in \check{\mathcal{W}}(-H_{ij} \underline{f}_{ij}, \underline{\pi}_i, \max\{\underline{\pi}_j, \underline{\pi}_i / \bar{r}_{ij}\}, \min\{\bar{\pi}_j, \underline{\pi}_i / \underline{r}_{ij}\}), \pi_i^{-4} = \underline{\pi}_i \lambda_{ij}^{-4}, f_{ij}^{-4} = \underline{f}_{ij} \lambda_{ij}^{-4} \\ (\pi_j^{-5}, -l_{ij}^{-5}, \lambda_{ij}^{-5}) \in \check{\mathcal{W}}(-H_{ij} \underline{f}_{ij}, \underline{\pi}_i, \max\{\underline{\pi}_j, \underline{\pi}_i / \bar{r}_{ij}\}, \min\{\bar{\pi}_j, \underline{\pi}_i / \underline{r}_{ij}\}), \pi_i^{-5} = \bar{\pi}_i \lambda_{ij}^{-5}, f_{ij}^{-5} = \underline{f}_{ij} \lambda_{ij}^{-5} \end{array} \right.$$

## References

- [1] IEA: Global Gas Security Review 2023. <https://www.iea.org/reports/global-gas-security-review-2023> (2023)
- [2] Ríos-Mercado, R.Z., Borraz-Sánchez, C.: Optimization problems in natural gas transportation systems: A state-of-the-art review. *Applied Energy* **147**, 536–555 (2015)
- [3] Gross, M., Pfetsch, M.E., Schewe, L., Schmidt, M., Skutella, M.: Algorithmic results for potential-based flows: Easy and hard cases. *Networks* **73**(3), 306–324 (2019)
- [4] Labbé, M., Plein, F., Schmidt, M., Thürauf, J.: Deciding feasibility of a booking in the European gas market on a cycle is in P for the case of passive networks. *Networks* **78**(2), 128–152 (2021)
- [5] Humpola, J.: Gas Network Optimization by MINLP. PhD thesis, Technische Universität Berlin (2014)
- [6] Wolf, D., Smeers, Y.: The gas transmission problem solved by an extension of the simplex algorithm. *Management Science* **46**(11), 1454–1465 (2000)
- [7] Ehrhardt, K., Steinbach, M.C.: Nonlinear optimization in gas networks. In: Bock, H.G., Phu, H.X., Kostina, E., Rannacher, R. (eds.) *Modeling, Simulation and Optimization of Complex Processes*, pp. 139–148. Springer, Berlin, Heidelberg (2005)
- [8] Steinbach, M.C.: On PDE solution in transient optimization of gas networks. *Journal of Computational and Applied Mathematics* **203**(2), 345–361 (2007). Special Issue: The first Indo-German Conference on PDE, Scientific Computing and Optimization in Applications
- [9] Schmidt, M.: An interior-point method for nonlinear optimization problems with locatable and separable nonsmoothness. *EURO Journal on Computational Optimization* **3**(4), 309–348 (2015)
- [10] Wu, Y., Lai, K.K., Liu, Y.: Deterministic global optimization approach to steady-state distribution gas pipeline networks. *Optimization and Engineering* **8**(3), 259–275 (2007)

- [11] Schmidt, M.: A Generic Interior-Point Framework for Nonsmooth and Complementarity Constrained Nonlinear Optimization. PhD thesis, Gottfried Wilhelm Leibniz Universität Hannover (2013)
- [12] Pfetsch, M.E., Fügenschuh, A., Geißler, B., Geißler, N., Gollmer, R., Hiller, B., Humpola, J., Koch, T., Lehmann, T., Martin, A., Morsi, A., Rövekamp, J., Schewe, L., Schmidt, M., Schultz, R., Schwarz, R., Schweiger, J., Stangl, C., Steinbach, M.C., Vigerske, S., Willert, B.M.: Validation of nominations in gas network optimization: models, methods, and solutions. *Optimization Methods and Software* **30**(1), 15–53 (2015)
- [13] Zhang, J., Zhu, D.: A bilevel programming method for pipe network optimization. *SIAM Journal on Optimization* **6**(3), 838–857 (1996)
- [14] Wu, S., Ríos-Mercado, R.Z., Boyd, E.A., Scott, L.R.: Model relaxations for the fuel cost minimization of steady-state gas pipeline networks. *Mathematical and Computer Modelling* **31**(2), 197–220 (2000)
- [15] Andre, J., Bonnans, F., Cornibert, L.: Optimization of capacity expansion planning for gas transportation networks. *European Journal of Operational Research* **197**(3), 1019–1027 (2009)
- [16] Babonneau, F., Nesterov, Y., Vial, J.-P.: Design and Operations of Gas Transmission Networks. *Operations Research* **60**(1), 34–47 (2012)
- [17] Fügenschuh, A., Humpola, J.: A Unified View on Relaxations for a Nonlinear Network Flow Problem. Technical Report 13-31, ZIB, Takustr. 7, 14195 Berlin (2013)
- [18] Wu, F., Nagarajan, H., Zlotnik, A., Sioshansi, R., Rudkevich, A.M.: Adaptive convex relaxations for gas pipeline network optimization. In: 2017 American Control Conference (ACC), pp. 4710–4716 (2017)
- [19] Ordoudis, C., Pinson, P., Morales, J.M.: An integrated market for electricity and natural gas systems with stochastic power producers. *European Journal of Operational Research* **272**(2), 642–654 (2019)
- [20] Borraz-Sánchez, C., Bent, R., Backhaus, S., Hijazi, H., Hentenryck, P.V.: Convex relaxations for gas expansion planning. *INFORMS Journal on Computing* **28**(4), 645–656 (2016)
- [21] Martin, A., Möller, M., Moritz, S.: Mixed integer models for the stationary case of gas network optimization. *Mathematical Programming* **105**(2-3), 563 (2006)
- [22] Zheng, Q.P., Rebennack, S., Iliadis, N.A., Pardalos, P.M.: Optimization Models in the Natural Gas Industry. In: Pardalos, P., Rebennack, S., Pereira, M., Iliadis, N. (eds.) *Handbook of Power Systems I. Energy Systems*. Springer, Berlin, Heidelberg (2010)
- [23] Wang, B., Yuan, M., Zhang, H., Zhao, W., Liang, Y.: An MILP model for optimal design of multi-period natural gas transmission network. *Chemical Engineering Research and Design* **129**, 122–131 (2018)
- [24] Ojha, A., Kekatos, V., Baldick, R.: Solving the natural gas flow problem using semidefinite program relaxation. In: 2017 IEEE Power Energy Society General Meeting, pp. 1–5 (2017)
- [25] Borraz-Sánchez, C., Bent, R., Backhaus, S., Blumsack, S., Hijazi, H., Hentenryck, P.: Convex optimization for joint expansion planning of natural gas and power systems. In: 2016 49th Hawaii International Conference on System Sciences (HICSS), pp. 2536–2545 (2016)
- [26] Wen, Y., Qu, X., Li, W., Liu, X., Ye, X.: Synergistic operation of electricity and natural gas networks via adm. *IEEE Transactions on Smart Grid* **9**(5), 4555–4565 (2018)
- [27] He, Y., Shahidehpour, M., Li, Z., Guo, C., Zhu, B.: Robust constrained operation of integrated electricity-natural gas system considering distributed natural gas storage. *IEEE Transactions on Sustainable Energy* **9**(3), 1061–1071 (2018)
- [28] Singh, M.K., Kekatos, V.: Natural Gas Flow Equations: Uniqueness and an MI-SOCP Solver. In: 2019 American Control Conference (ACC), pp. 2114–2120 (2019)
- [29] Schewe, A., Ordoudis, C., Kazempour, J., Pinson, P.: Coordination of power and natural gas systems: Convexification approaches for linepack modeling. In: 2019 IEEE Milan PowerTech, pp. 1–6 (2019)

- [30] Li, Y., Dey, S.S., Sahinidis, N.V.: A reformulation-enumeration minlp algorithm for gas network design. *Journal of Global Optimization* **90**(4), 931–963 (2024)
- [31] Burlacu, R., Egger, H., Groß, M., Martin, A., Pfetsch, M.E., Schewe, L., Sirvent, M., Skutella, M.: Maximizing the storage capacity of gas networks: a global minlp approach. *Optimization and Engineering* **20**(2), 543–573 (2019)
- [32] Borraz-Sánchez, C., Ríos-Mercado, R.Z.: Improving the operation of pipeline systems on cyclic structures by tabu search. *Computers & Chemical Engineering* **33**(1), 58–64 (2009)
- [33] Koch, T., Pfetsch, M.E., Schewe, L.: Evaluating Gas Network Capacities. MOS-SIAM Series on Optimization, SIAM, Philadelphia (2015)
- [34] Osiadacz, A.: Simulation and Analysis of Gas Networks. Gulf Publishing Company, Houston, TX (1987)
- [35] Tuncer, D., Kocuk, B.: An MISOCP-Based Decomposition Approach for the Unit Commitment Problem With AC Power Flows. *IEEE Transactions on Power Systems* **38**(4), 3388–3400 (2023)
- [36] McCormick, G.P.: Computability of global solutions to factorable nonconvex programs: Part i —convex underestimating problems. *Mathematical Programming* **10**(1), 147–175 (1976)
- [37] Tawarmalani, M., Richard, J.-P.P.: Decomposition techniques in convexification of inequalities. Technical report, Technical report (2013)
- [38] Hillestad, R.J., Jacobsen, S.E.: Linear programs with an additional reverse convex constraint. *Applied Mathematics and Optimization* **6**, 257–269 (1980)
- [39] Ben-Tal, A., Nemirovski, A.: Lectures on Modern Convex Optimization: Analysis, Algorithms, and Engineering Applications. SIAM-MOS Series on Optimization, SIAM, Philadelphia (2001)
- [40] Matthias, M.: mittelmann-plots - Visualizations of Mittelmann benchmarks. <https://mattmilten.github.io/mittelmann-plots/> (2024)
- [41] A Library of Gas Network Instances. <http://gaslib.zib.de>. Online, 2024
- [42] Hennings, F.: Modeling and solving real-world transient gas network transport problems using mathematical programming. PhD thesis, Technische Universität Berlin (2023)
- [43] Gurobi Optimization, L.: Gurobi Optimizer Reference Manual. [www.gurobi.com/documentation/](http://www.gurobi.com/documentation/) (2024)
- [44] Wächter, A., Biegler, L.T.: On the implementation of an interior-point filter line-search algorithm for large-scale nonlinear programming. *Mathematical Programming* **106**(1), 25–57 (2006)
- [45] Tawarmalani, M., Sahinidis, N.V.: A polyhedral branch-and-cut approach to global optimization. *Mathematical Programming* **103**(2), 225–249 (2005)